Title: Indian Hedgehog release from TNF activated renal epithelia drives local and remote organ fibrosis

Authors: Eoin D O'Sullivan[1,2°], Katie J Mylonas[1°], Cuiyan Xin[3°], David Baird[1], Cyril Carvalho[1], Marie-Helena Docherty[1], Ross Campbell[1], Kylie P Matchett[1], Scott H Waddell[4], Alexander Walker[4], Kevin M Gallagher[1,5], Siyang Jia[1], Steve Leung[5], Alexander Laird[5], Julia Wilflingseder[2,6], Michaela Willi[7], Maximillian Reck[8], Sarah Finnie[8], Angela Pisco[9], Sabrina Gordon-Keylock[10], Alexander Medvinsky[10], Luke Boulter[4], Neil C Henderson[1,4], Kristina Kirschner[11,12], Tamir Chandra[4], Bryan R Conway[8], Jeremy Hughes[1], Laura Denby[8], Joseph V Bonventre[3], David A Ferenbach[1,3*]

Affiliations:

[1]Centre for Inflammation Research, Queen's Medical Research Institute, University of Edinburgh, Edinburgh, EH16 4TJ ,UK.

[2]Kidney Health Service, Royal Brisbane and Women's Hospital, Brisbane, Queensland, 4029, Australia.

[3]Renal Division and Division of Engineering in Medicine, Brigham and Women's Hospital, Department of Medicine, Harvard Medical School, Boston, MA, 02115, USA.

[4]MRC Human Genetics Unit, Institute of Genetics and Cancer, University of Edinburgh, Edinburgh, EH4 2XU, UK.

[5]Department of Urology. Western General Hospital, Edinburgh, EH4 2XU, UK.

[6]Department of Physiology and Pathophysiology, University of Veterinary Medicine, Veterinärplatz 1, 1210 Vienna, Austria.

[7]Laboratory of Genetics and Physiology, NIDDK, NIH, Bethesda, MD, 20892, USA

[8]Centre for Cardiovascular Science, Queen's Medical Research Institute, University of Edinburgh, Edinburgh, EH16 4TJ, UK

[9]Chan Zuckerberg Biohub, San Francisco, CA, 94158, USA.

[10]Centre for Regenerative Medicine. University of Edinburgh, Edinburgh, EH16 4UU, UK.

[11]School of Cancer Sciences, College of Medical, Veterinary and Life Sciences, University of Glasgow, Glasgow, G12 8QQ, UK.

[12]Cancer Research UK Beatson Institute, Glasgow, G61 1BD, UK

°denotes equal contribution, *Corresponding author

One Sentence Summary: Indian Hedgehog release from TNF-activated renal epithelia drives proliferation and activation of Gli1 expressing cells, linking inflammation to fibrosis.

Abstract:

Progressive fibrosis is a feature of aging and chronic tissue injury in multiple organs including the kidney and heart. Glioma associated oncogene 1 expressing (Gli1+) cells are a major source of activated fibroblasts in multiple organs but the links between injury, inflammation and Gli1+ cell expansion and tissue fibrosis remain incompletely understood. We demonstrated that leukocyte-derived tumour necrosis factor (TNF) promoted Gli1+ pericyte/fibroblast proliferation and cardio-renal fibrosis through induction and release of Indian Hedgehog (IHH) from renal epithelial cells. Using single cell resolution transcriptomic analysis we identified an 'inflammatory' proximal tubular epithelia (iPT) population contributing to TNF and NF-κB induced IHH production in vivo. TNF-induced Ubiquitin D (*Ubd)* expression was observed in human proximal tubular cells in vitro and during murine and human renal disease and aging. Studies using pharmacological and conditional genetic ablation of TNF induced IHH signalling revealed that IHH activated canonical Hedgehog signalling in Gli1+ cells, which led to their activation, proliferation and fibrosis within the injured and aging kidney and heart. These changes were inhibited in mice by *Ihh* deletion in *Pax8* expressing cells or pharmacological blockade of TNF, NFκB or Gli1 signalling. Increased amounts of circulating IHH were associated with loss of renal function and higher rates of cardiovascular disease in patients with chronic kidney disease. Thus, Indian Hedgehog connects leukocyte activation to Gli1+ cell expansion and represents a potential target for therapies designed to inhibit inflammation-induced fibrosis.

Main Text:

Introduction

Physiological aging is associated with increased amounts of baseline organ fibrosis and increased expression of inflammatory cytokines including IL-6 and tumour necrosis factor (TNF) (*1, 2*). Immune activation is also present in aging-related illnesses such as chronic kidney disease (CKD) (*3-5*). Of note, patients with CKD exhibit accelerated cardiovascular disease and fibrosis, with CKD implicated in premature cardiovascular aging (*6*). Furthermore, the persistence of leukocytes within the injured kidney has been shown to correlate with progressive fibrosis in animal disease models (*7*) and human CKD (*8*). The association between leukocytes and fibrosis remains present in diseases without an auto-immune aetiology, and settings in which injury has apparently resolved, such as previous acute kidney injury (AKI) (*4*). Recent prospective clinical studies and cohort analysis have demonstrated that AKI is associated with increased long-term risks of subsequent cardiac failure and death (*9, 10*). It has been proposed that leukocytes contribute to maladaptive repair, kidney fibrosis and cardiovascular disease in both aging and CKD (*11*). Whilst experimental evidence suggests a link between the prototypic inflammatory cytokine TNF and renal fibrosis (*12-14*) the underlying mechanism remains incompletely understood.

Recent research has focused on identifying the cells primarily responsible for organ fibrosis. In both the kidney and heart, it has been shown that the majority of injury-induced fibrosis is produced by proliferation and activation of resident mesenchymal cells that express the Gli1 transcription factor. These cells include pericytes and fibroblasts and are typically present at low numbers in healthy organs (*15-18*). While the key role of proliferation of perivascular Gli1 labelled cells in organ fibrosis has been established(*17*), the upstream signalling pathways

responsible for the activation of the Gli1 and Gli2 transcription factors leading to their expansion remain incompletely characterised (*19*).

Published work implicates renal epithelia as regulators of injury outcome via interactions with leukocytes, endothelia and myofibroblasts (*20-22*). Examining the aftermath of renal injury, several groups have reported new epithelial subsets (*23*), including single cell resolution analysis of populations with evidence of NFκB activation (*24, 25*) which has been previously been implicated in kidney injury (*26*). However, the potential connections between TNF(*12*), epithelial NFκB (*27*) and organ fibrosis are unclear.

In this study we hypothesized that signalling from epithelial cell subsets within the kidney activated Gli1+ pericytes/fibroblasts and induced fibrosis. Using new and recently published single cell datasets of fibrotic and aged kidneys we identified a subset of Ubiquitin D (Ubd)-expressing renal epithelial cells that produce Indian Hedgehog (IHH) in response to activation by TNF signalling from leukocytes. We demonstrated that selective genetic and pharmacologic inhibition of this TNF, NFκB and IHH-dependent pathway led to reduced tissue fibrosis and reduced proliferation of Gli1+ pericytes/fibroblasts in the kidney and heart independent of kidney function or blood pressure. We also found that $UBD^{+}IHH^{+}$ epithelial cells were present in human kidney disease and that increased circulating IHH correlated with cardiovascular disease and renal functional loss in patients. Collectively these results suggest TNF release from activated leukocytes can lead to tissue fibrosis and provide novel targets for anti-fibrotic therapies.

Results

Ubd^{+} renal epithelia are present in aged and fibrotic kidneys in mice

First, we investigated whether distinct renal epithelial populations were responsible for fibrotic signalling after injury or during aging. We performed single cell RNA sequencing (scRNAseq) on control and fibrotic kidneys from young (6-8 week old) mice 6 weeks after unilateral ischaemia-reperfusion injury (uIRI) (Fig. 1A, S1A-D). To characterize the impact of age on renal fibrosis, we also examined the *Tabula Muris Senis* (*TMS*) database (*28*) for aging-associated renal epithelial clusters (Fig. 1B S2A-C). One distinct cluster of proximal tubule epithelial cells was detected using Seurat's FindClusters function in young fibrotic kidneys which we classified as "inflammatory" proximal tubule (iPT) based on its gene expression profile, including Differentially Expressed transcripts for chemokine (C-C motif) ligand 2 (*Ccl2*), Transcription factor *RelB* and Intracellular Adhesion Molecule 1 (*Icam1*) (Fig. 1C,E, S1A-D).

An epithelial cluster expressing multiple shared genes with post-injury iPTs was also detected in uninjured aging kidneys through analysis of 21,647 renal cells from the *TMS* dataset (Fig. 1B, S2A-C). In 1-3 month old mice, this cluster comprised 1.4% of epithelia but had increased to 12% in 18-30 month-old mice, Fig. 1D,F Fig. S2C). Whilst iPT cells expressed several markers indicating that they originated from proximal tubular epithelial cells, including LDL Receptor Related Protein 2 (*Lrp2*) and solute carrier family 27 member 2 (*Slc27a2*), additional transcriptional differences separated iPT clusters from other epithelia in fibrotic and aged kidneys (Fig. 1E-F, Fig. S2A-C, S3, S4). 3 notable transcript changes in iPT cells were increased expression of Ubiquitin D (*Ubd*), Prostaglandin D2 Synthase (*Ptgds*) and CCN Family Member 1 (CCN1/*Cyr61* (*29*)). iPT cells also expressed increased Vascular Cell

Adhesion molecule 1 (*Vcam1)*, which in addition to its role in the vasculature has been proposed to identify proximal tubular epithelia with increased NF-κB activation (*25*). Colocalization of *Ubd* and *Vcam1* in a subset of renal epithelial cells was also identified by in situ hybridization after uIRI (Fig S5A).

Using UBD as a marker of iPT cells we also explored human datasets for evidence of altered *UBD* expression in the kidney with aging. Work by Rodwell et al (*30*) showed a positive association between increasing age and renal UBD expression. In this study, we found UBD+ cells were increased in human kidneys with the highest amounts of interstitial fibrosis, glomerular and tubular atrophy (Fig S5B).

TNF and NF-κB signalling pathways are activated in *Ubd*+ iPT cells in kidney injury and aging in mice

The presence of iPT cells in uninjured aged murine kidneys indicated that this epithelial subset existed in the absence of tissue injury. We examined expression of known TNF-responsive genes (*31*) in both datasets and found multiple of these targets were increased in iPT cells with aging or injury (Fig. 1E,F). Upregulated *Ubd* and *Cxcl16* expression were both consistent with iPT cells responding to TNF stimulation (*32, 33*). Previous work has demonstrated that leukocytes are the major source of renal TNF (*34*). We found that *Tnf* transcript expression in control and fibrotic kidneys was confined to leukocytes in both young fibrotic and aged kidneys (Fig. S5C-D). Over representation analysis demonstrated enrichment of TNF and downstream NFκB signalling pathways in iPT clusters (Fig. 1G-H). We therefore explored the potential role of TNF and *Ubd*+ iPT cells in aging and injury-induced renal fibrosis.

TNF/NF-κB signalling induces *Ubd* expression in renal epithelia in vitro and is profibrotic in vivo

To determine whether TNF alone was sufficient to induce *Ubd* and clarify the role of NFκB signalling in this process, TNF was added to human renal proximal tubular cells (RPTECs) cultured in vitro ± the NFκB inhibitor BAY 11-7082 (Fig. S6A). TNF exposure led to increased *Ubd* expression in proximal tubular cells that was dependent on NFκB signalling (Fig. S6B).

We then examined the role of TNF in fibrosis in vivo using the clinically licenced TNF inhibitor Infliximab. First, we tested the effects of Infliximab on renal ischaemia-reperfusion injury (Fig. 2A). Consistent with a profibrotic role for TNF, mice had less interstitial fibrosis, Collagen I deposition, alpha-smooth muscle actin (αSMA+) myofibroblast expansion and increased renal mass 3 weeks after uIRI with TNF antagonism (Fig. 2B,C). In situ hybridisation (ISH) to *Ubd* and *Col1a1* demonstrated upregulation of *Ubd* in proximal tubules after injury, often adjacent to *Col1a1* expressing interstitial cells. *Ubd*+ cells were reduced five-fold compared to baseline with TNF antagonism, consistent with the hypothesis that TNF promoted *Ubd* expressing iPT cells in vivo (Fig. 2D). We next tested Infliximab in another type of renal injury, unilateral ureteric obstruction (UUO), in aged mice (Fig. 2E). TNF antagonism again reduced tissue fibrosis after UUO (Fig. 2F) and prevented the upregulation of *Ubd* seen after 7 days after injury by qPCR (Fig. S6C). Collectively, these findings suggested iPT epithelial cells were responsive to TNF and NFκB signaling and contributed to renal fibrosis. To determine whether NFκB activation was necessary for TNF-induced fibrosis, uIRI mice were treated with Bortezomib, a proteasome inhibitor that stabilizes the endogenous NFkB inhibitor IκBα, thus inhibiting NFkB (in addition to widespread alteration in protein breakdown via its inhibition of the 26S proteasome(*35*)). We found NFκB inhibition also reduced post-injury fibrosis, collagen I deposition and αSMA+ myofibroblast accumulation (Fig 3A-C).

TNF induced NFκB activation results in *Ihh* transcription by iPT cells in vitro, ex vivo and in vivo

qPCR performed on kidneys from our murine uIRI and UUO disease models demonstrated that *Icam1*, *Sox9* (*36*), *Ihh* and *Col1a1* transcripts were all reduced with Infliximab, whilst *Tgfb1* remained unchanged (Fig. 3D). Consistent with the necessity of NFκB activation for *Ihh* production and subsequent fibrosis, NFκB inhibition with Bortezomib also reduced the post-injury upregulation in *Icam1*, *Ihh* and *Col1a1* transcripts, despite maintained expression of *Ubd*, suggesting *Ubd* expression was regulated upstream or independently of NF-κB(Fig 3E).

To determine the mechanism connecting TNF to tissue fibrosis we returned to our scRNAseq datasets to examine pathways known to be activated in renal disease (*37*). Although published work has implicated epithelial Sonic Hedgehog (*Shh)* induction as a key driver of kidney fibrosis in vivo (*38*), this was not differentially expressed in iPT cells in young fibrotic kidneys, or in the kidneys from aged mice in the TMS database (Table S1A,B and GEO online data). When exploring the entire *TMS* database, *Shh* expression was largely confined to bladder epithelia and did not increase with age in renal epithelia (Fig. S7). *Ihh* was the sole Hedgehog transcript highly expressed by any renal cell, with *Ihh* and *Tgfb2* differentially expressed in iPT cells (Fig. 1B, C, Table S1A-B and GEO online data). We reviewed datasets from our recent published work (*39*) and found *Ihh* expression rose in the kidney at day 2 post-UUO (where profibrotic signalling is known to be induced and leukocyte *Tnf* production maximal) and fell alongside *Acta2* and *Col3a1* in our model of 'Reversed UUO' where the obstruction had been removed and leukocyte *Tnf* signalling and fibrosis are known to be reduced (Fig. S8A-B). In contrast no elevation was seen in *Shh* expression after injury (Fig. S8C). These findings supported a role for *Ihh* but not *Shh* in renal fibrosis. In situ hybridization on uninjured young

and aged murine kidneys also demonstrated *Ubd* and *Ihh* co-localisation could be found within aged proximal tubules (Fig. S8D).

To explore any connection between TNF and IHH production in human kidneys, we examined precision cut kidney slices from cancer-free renal tissue obtained during cancer nephrectomy surgery (Fig S8E). We found *ICAM1*, *UBD* and *IHH* all rose more than 3-fold after 24h of TNF treatment compared to vehicle alone (Fig S8F).

Given that Hh can promote collagen synthesis in fibroblasts similar to TGF-β in vitro (*40*) we tested the ability of Hh ligands to -activate TGF-β signalling. Western blotting indicated that Hh ligands did not induce phosphorylation of SMAD3 and therefore promoted fibrosis independent of the canonical TGF-β pathway (Fig S8G,H).

Renal epithelial *Ihh* production drives kidney fibrosis in two models of renal injury

To determine the role of *Ihh* in post-injury fibrosis we generated transgenic mice to delete *Ihh* conditionally in renal epithelial cells. The *Pax8* transcription factor was highly expressed in iPT cells so Pax8-CreERT2;Ihh$^{fl/fl}$ were generated to allow inducible deletion of *Ihh* in Pax8 expressing cells with tamoxifen administration (Fig. 4A, confirmed by ISH). The expression of Pax8 has been documented to be restricted to renal epithelia with no expression in skin, fat, pancreas, stomach, small and large intestine, spleen, liver, bladder, genital tract, thymus, heart, lungs, muscle, salivary glands, thyroid, brain, and bone (*41*). We used a conditional approach since constitutive *Ihh* deletion is lethal (*42*). Tamoxifen treated Pax8-CreERT2;Ihh$^{fl/fl}$ mice developed less fibrosis at d7 post UUO compared to vehicle treatment or tamoxifen treated transgenic and non-transgenic mice (Fig. 4B-C). These data indicated *Ihh* in renal epithelial cells contributed to fibrosis.

Unilateral IRI was performed in Pax8-CreERT2;Ihh$^{fl/fl}$ mice and non-transgenic littermates. Both wild-type and Pax8-CreERT2;Ihh$^{fl/fl}$ mice received tamoxifen 2 weeks before and 1 week after uIRI while control animals received vehicle without surgery (Fig. 4D). Measurement of kidney weight and fibrosis demonstrated increased renal size and reduced fibrosis in kidneys with epithelial *Ihh* depletion compared to wild type kidneys receiving matched dose tamoxifen (Fig. 4E). Reductions in renal *Ihh* transcript expression were seen in injured kidneys from Tamoxifen treated transgenic mice (adj $p<0.05$ vs WT IRI+TAM). Over-representation analysis of bulk RNA-Seq data showed reductions in multiple pathways including Hedgehog signalling in epithelial *Ihh* depleted kidneys compared to wild-type, despite maintained *Shh* expression (Fig. 4F). Comparison of post-uIRI kidneys with epithelial *Ihh* depletion to those with intact epithelial *Ihh* demonstrated no change in upstream TNF, TGF-β signalling, *Shh* or markers of iPT induction (*Tnf*, *Tgfb1, Tgfb2*, *Ctgf, Ubd* and *Vcam1*, all adj p=NS, Table S1C and GEO online data). In contrast, *Ihh* expression and downstream markers of myofibroblast proliferation and activation were significantly reduced (*Ihh*, *Acta2*, *Pdgfra*, *Col1a1* and *Col3a1* all adj $p<0.05$, Table S1C and GEO online data). RNAseq analysis demonstrated no evidence of upregulated *Ihh* expression in either the contralateral kidney or heart in WT mice undergoing IRI vs Naïve mice (Log2FC -0.28 and Log2FC -0.39 respectively, Adj $p>0.5$ in both cases).

IHH^{+}*UBD*$^{+}$ iPT cells are present in aged and diseased human kidneys

We also performed *ISH* for IHH and UBD expression in human kidney tissue from young and aged kidneys pre-transplantation, and from a human kidney biopsy with progressive IgA nephropathy. In both a 'healthy' aged kidney awaiting transplantation and a biopsy from a kidney with IgA nephropathy renal epithelia co-expressing IHH and UBD were identified

which were not present in young non-diseased control kidney (Fig. 5A, Fig. S8I). These preliminary data suggest *IHH*$^{+}$*UBD*$^{+}$ iPT cells exist in humans.

Circulating IHH protein is increased in patients with progressive CKD

We next tested whether patients with renal pathologies considered 'high risk' for progressive fibrosis in the kidney and heart (IgA and diabetic nephropathy) had higher amounts of circulating IHH protein compared to patients with 'low risk' renal diagnoses. 'Low risk' diagnoses included those associated with proteinuria (Minimal Change glomerulonephritis) and functional loss not usually associated with progressive fibrosis (unilateral nephrectomy). Patients with 'high risk' CKD had serum IHH concentrations 3x higher than those with 'low risk' disease, and lost function 5 times more quickly over the next >2.5 years (Fig. 5B). Examining the entire dataset and patients confined to the 'high risk' subset only showed that patients with incident or prevalent cardiovascular disease had >3 fold higher circulating IHH in both cases (Fig. 5B).

Induction of canonical Hedgehog signalling is profibrotic in the healthy young murine kidney

To confirm whether activation of canonical Hedgehog signalling through Smoothened was sufficient to induce fibrosis in the absence of other profibrotic stimuli in vivo, young healthy mice were dosed for 7 days with Smoothened Agonist (SAG, Fig. 6A). Treatment with SAG induced fibrosis in the kidney as well as perivascular regions of the heart (Fig. 6B), which are known to contain Gli1+ cells (*17*). Immunofluorescence staining showed increased Collagen I with SAG treatment in renal perivascular regions (Fig S9A, $p<0.05$) in the absence of leukocyte recruitment or αSMA^{+} myofibroblast accumulation (Fig S9B-C). Thus, canonical Hedgehog signalling appeared to be sufficient to drive fibrosis in the kidney as well as the heart, which

agrees with published work reporting the ability of a renal limited injury to induce fibrosis in remote organs (*43*).

Pharmacological inhibition of Gli1/2 signalling inhibits renal fibrosis post injury

Next, we explored the contribution of Gli1 signalling to kidney fibrosis after IRI using an inducible, Gli1-driven TdTomato reporter mouse and the Gli1/2 antagonist GANT61 (Fig 6C). Picrosirius Red (PSR) measurement of total fibrosis deposition (Fig 6D, $p<0.05$) and immunofluorescent staining for Collagen I (fig. S10A, $p<0.001$) at 6 weeks post IRI showed significant reductions in GANT61 treated mice. This coincided with a reduction in TdTomato labelled cells, which indicated reduced expansion of Gli1 expressing progenitors despite comparable numbers of αSMA+ myofibroblasts (Fig 6E, fig. S10B). qPCR assessment of renal tissue confirmed inhibition of Gli1/2 target genes (*Snai1* and *Cxcl4*) and reduced expression of *Col1a1* and *Col3a1* transcripts despite unaltered *Ubd, Tgf* and *Acta2* (Fig S10C).

IHH is a non-redundant mediator of TNF signalling induced fibrosis post-injury

We then tested the ability of TNF signalling inhibition to preserve kidney function and limit fibrosis after injury was established in a bilateral renal ischaemia reperfusion model (bIRI) (Fig 6F). Tamoxifen-treated WT or Pax8-CreERT2;$Ihh^{fl/fl}$mice were compared to mice with TNF inhibition (Infliximab) or canonical Hh inhibition (GANT61) starting 24h after injury. TNF inhibition was also combined with genetic ablation of epithelial *Ihh* expression to examine potential additive effects. Pharmacological inhibition of TNF signalling reduced kidney fibrosis and preserved kidney function comparably to epithelial Ihh knockdown (Fig. 6G-I). The addition of TNF blockade to animals already lacking epithelial *Ihh* elicited no additional protection, which suggested a non-redundant role for IHH in TNF mediated profibrotic signalling.

Renal injury induces transcriptional changes in remote organs in the absence of hypertension

We wanted to determine if localized renal injury could negatively impact its contralateral partner remotely. Bulk RNAseq analysis demonstrated that in mice injured 10 weeks previously by uIRI, the uninjured kidney also upregulated inflammatory signalling and collagen transcripts compared to a mouse with a single uninjured kidney 10 weeks after a contralateral nephrectomy (with equivalent or lower GFR). Thus, previous renal injury appeared to mediate systemic effects independent of renal functional loss (Fig. S11).

Hypertension and reduced renal clearance of waste products have both been proposed to contribute to the increased incidence of cardiac fibrosis in experimental and human CKD (*44-46*). To explore this, we returned to our model of transgenic *Ihh* depletion in Pax8 expressing renal epithelial cells. There was no change in Ihh expression in hearts of tamoxifen treated transgenic mice as compared to tamoxifen treated wild type controls (Log2FC 0.009, adj p=1). No cardiac cells expressing Pax8 were seen in the TMS dataset (Fig S12A), consistent with *Ihh* deletion in our Pax8-Cre mice being specific to renal epithelia. Using this model we analysed whether uIRI to a single kidney induced perivascular cardiac fibrosis without advanced renal impairment (due to the presence of an uninjured contralateral kidney). Blood pressure readings taken before, 1 week after and 10 weeks after injury showed that unilateral IRI did not induce hypertension in any group (Fig. 7A, B). Despite this, measurement of the well validated heart weight to tibial length ratio (*47*) and perivascular fibrosis demonstrated cardiac fibrosis still occurred in the absence of hypertension or advanced renal impairment, but was reduced in the absence of Pax8+ epithelial *Ihh* production (Fig. 7B). This finding was compatible with the published reports of increased Hedgehog signalling promoting fibroblast proliferation within

the heart independent of blood pressure changes (*48, 49*). Echocardiography of a subset of each group demonstrated preserved cardiac function across all groups, with significant LV mass increase in *Ihh* WT mice post uIRI compared to unilateral nephrectomy only ($p<0.05$) that was not present in Pax8-CreERT2;$Ihh^{fl/fl}$ mice post uIRI (Table S2). We examined the data from the *TMS* database and found markers of Hh activation in cardiac fibroblasts from aged mice despite minimal *Ihh* and absent *Shh* transcript production in any cardiac cell type (Fig. S12A). These findings supported the hypothesis that circulating hedgehog ligands can induce remote fibrosis, consistent with recent reports of raised systemic Hh signalling in human patients with renal failure (*50*).

Renal injury results in long term leukocyte infiltration and activation in the kidney

The prototypic T and B lymphocyte (*Cd3g* and *Cd19*) and macrophage transcriptional markers (*Adgre1* and *Cd68)* all remained significantly upregulated at 10 weeks post injury in the injured kidney compared to naïve controls (adj p=0.012, 0.003, 2.64×10^{-7} and 1.02×10^{-5} respectively, Table S1D and in GEO online data). In contrast, none of these markers were elevated in hearts from animals with injured kidneys vs uninjured controls or in contralateral kidneys vs uninjured controls (Table S1E-F and in GEO online data). These findings were confirmed by flow cytometric analysis of post-uIRI, contralateral and naïve kidneys and hearts (Fig S12B). These data suggested that the systemic fibrotic response in distant organs was not dependent on inflammation from local cellular infiltrates. Additional analysis of M1 and M2 macrophage activation markers in post-uIRI compared to naïve kidneys found the most significantly upregulated transcript was *Mrc1* (CD206 – a prototypic marker of M2 macrophages, (Adj $p=4.70 \times 10^{-7}$). However, markers of M1 macrophage polarisation were also significantly upregulated (*Cxcl10*, *Nos2*, Adj p=0.0001 & 0.009 respectively, Table S1D and in GEO online

data). Thus, transcriptomic evidence supported the accumulation and persistence of both M1 and M2 macrophage subsets in injured kidney.

Pharmacological inhibition of Hh signalling inhibits remote fibrosis after kidney injury

We next examined the effect of GANT61 inhibition on remote organ fibrosis in our uIRI model. By only injuring one kidney we could assess effects on both the uninjured contralateral kidneys and hearts (Fig. 7C). At 6 weeks post-uIRI, fibrosis (PSR staining and Collagen I immunofluorescence) and expansion of Gli1+ pericytes/fibroblasts and αSMA+ myofibroblasts were increased in the injured kidney (Fig 6C-F, S10A-B). Similar changes were seen in contralateral kidneys and hearts of vehicle treated post-uIRI animals compared to animals undergoing unilateral nephrectomy, an effect lost with Gli1 inhibition (Fig. 7D-E). Of note, mice undergoing unilateral nephrectomy did not develop subsequent contralateral kidney fibrosis despite the induction of an equal/larger functional decrease and increase in single kidney workload. Post-uIRI animals had the highest perivascular fibrosis in hearts and uninjured kidneys, with GANT61 mediated inhibition of Hedgehog signalling blocking fibrosis in both organs (Fig. 7D-E). Assessment of hearts was performed in the same Gli1-Ai14 mice where Gli1+ pericytes/fibroblasts were labelled before injury with Tamoxifen in all groups. We observed a major expansion of Gli1 derived cells in perivascular and interstitial regions at 6 weeks post injury that were note seen in mice undergoing nephrectomy only or from uIRI mice treated with GANT61 (Fig 7F).

To determine if the expansion of Gli1 derived cells was due to expansion of tissue resident precursors or recruitment of circulating bone marrow derived cells, murine bone marrow transplants were performed with strain matched WT and ROSA26-Cre;cCAG-Ai14 mice that constitutively express TdTomato (Fig S13A-B). We saw increases in total Pdgfrα^{+} activated

fibroblasts in both the kidney and heart after uIRI (Fig S13C-D). In the kidney >80% of CD45+ leukocytes and less than 4% of activated Pdgfra+ fibroblasts were TdTomato positive (Fig S13E), whilst less than 2% of cells in the heart were TdTomato+ (Fig S13F). These data demonstrated that >95% of fibroblasts in both organs derived from tissue resident cells.

Discussion

Chronic kidney disease affects hundreds of millions of people worldwide and is a major risk factor for accelerated cardiovascular disease and premature death (*51, 52*). Chronic inflammation is a feature common to all advancing kidney disease, but the mechanism to explain their connection remains incompletely understood. Here we show evidence that changes in the renal epithelial phenotype may link aging and inflammation to fibrosis.

We explored aging and injured kidneys from humans and mice at single cell resolution and identified a renal epithelial cell subset that produced *Ihh* in response to TNF. This cluster upregulated *Ubd, Vcam1, Sox9* and *Dcdc2a* and therefore may overlap with cells identified by other groups as 'failed-repair', 'new-PT1' or 'pro-inflammatory' epithelia after injury (*24, 53-55*). Of importance, using human cell culture, murine experimental kidney disease and human kidney biopsies we demonstrated that IHH can promote fibrosis in the kidney and heart through TNF, NFκB and Hedgehog signalling through Gli1+ cells in both organs (summarised in Figure S14). Collectively, these data link the immune activation present in aging, inflammation and organ injury (*1-3*) to progressive fibrosis (*6, 7*).

Published work supports the importance of Hedgehog signalling in renal fibroblasts in rodent models of CKD (*38*), which has been attributed to elevated Sonic Hedgehog protein in tubular epithelial cells after injury (*38, 56*). Using our own scRNAseq datasets we did not see upregulation of *Shh* after experimental renal injury. Instead, the profound reduction in collagen deposition seen in animals lacking *Ihh* but preserved *Shh* gene function supported a previously underappreciated role of *Ihh* as a fibrotic mediator. The identification of *Ihh* rather than *Shh* as a mediator of Gli1+ associated fibrosis was of therapeutic as well as mechanistic interest. Given

the tissue restricted expression of *Ihh*, it may be possible to design targeted therapies to limit fibrosis without the side effects typically associated with systemic inhibition of TNF or NFκB signalling.

Our data is consistent with studies performed in experimental rodent and human liver disease (*57-59*), showing that injury induced release of Hedgehog ligands from epithelia leads to hepatic myofibroblast activation. Studies in other organs in humans, mice, zebrafish, and fruit flies also support the ability of Hedgehog signalling to drive local and remote tissue development, cancer and post-injury fibrosis (*60-65*). The literature on cardiac Hedgehog signalling has focused mainly on the beneficial impact of Hedgehog signalling in cardiac development and on successful scar formation in the first 7 days after myocardial infarction (*66*). This is consistent with reports of acute endogenous upregulation of Hedgehog signalling being an important mediator of recovery after acute, limited liver injury (*67*). Importantly, in the liver longer term upregulation of Hh ligand expression within hepatocytes is present in progressive fibrosis (*59*), and cirrhosis (*68*) –consistent with the longer term outcomes addressed in our study. Reports have implicated even acute Hedgehog signalling in the heart as profibrotic, with inhibition of Hedgehog signalling resulting in less cardiac fibrosis with no deleterious impact on ejection fraction (*69*). It remains possible that the differences between our kidney studies and short- term studies in the heart reflect contrasting effects of early versus sustained Hedgehog signalling on the vasculature (where proliferation is beneficial) and the mesenchyme (where proliferation promotes fibrosis). Further studies are required to clarify the impact of timing, environment and injury on Hedgehog signalling in these settings.

Our findings regarding cardiac perivascular fibrosis and TNF-dependent Hedgehog signalling are consistent with published work showing that TNF knockout mice are protected from end

organ damage in models of hypertension (*70*) and with clinical studies in bone disease identifying *Ihh* as a TNF target (*71*). They are also compatible with the documented increases of perivascular fibrosis in the hearts of elderly patients and those with CKD, resulting in impaired coronary blood flow and susceptibility to myocardial hypoxia (*72-74*), although this has not been specifically linked to Hh or IHH. Previous work has focused on the beneficial impact of Sonic Hedgehog administration on cardiomyocyte and endothelial proliferation in the immediate aftermath of ischaemic injury (*49*). Our data raises concerns that prolonged agonism or elevated activity of circulating Hedgehog ligand may worsen cardiac fibrosis in Gli1+ cells – with fibrosis associated with reduced survival in patients with CKD (*6*). It is noteworthy that serum IHH was higher in patients with progressive CKD and cardiovascular disease in our study (Fig 3H). Our results are consistent with the reported impact of Hedgehog signalling on cardiac fibroblast proliferation (*49*), where acute SHH administration led to expanded αSMA positive fibroblast staining.

The current study has limitations. *Ihh* is minimally expressed in various epithelial cell subtypes in the healthy young kidney, and our single cell data demonstrates that iPT cells are the highest expressing, but not the only site of *Ihh* expression in the aftermath of injury. In addition to the pharmacological interventions on UUO in aged mice presented here it will be valuable to assess the long-term impact of IHH on renal homeostasis, physiological aging and injury responses. Additionally, while no murine model can fully replicate the multiple pathologies contributing to human kidney disease, our studies provide evidence that perivascular cardiac fibrosis could occur in the absence of cardiac dysfunction during the timeframes studied here. It is noteworthy that in mice with preserved renal epithelial IHH, cardiac perivascular fibrosis occurred despite equivalent renal function and blood pressure to mice undergoing contralateral nephrectomies

alone, suggesting that neither of these factors appear to be necessary for the initiation of this important disease process.

Whilst our transgenic studies implicate Ihh release from injured epithelial cells as a key driver of multi-organ fibrosis – further studies are required to assess whether other factors contribute to extra-renal fibrotic outcomes. In human disease perivascular fibrosis is associated with myocardial ischaemia and worsened outcomes after cardiac events (*75*). Further studies focusing on experimental cardiac injury and repair prior to larger, prospective studies in human disease will be required to validate and extend the work presented here. CKD is associated with increased cellular exosome release (*76*). IHH can be secreted within circulating exosomes (*77*) so it is possible that the increases in total circulating IHH in CKD were even larger than those detected by serum ELISA. It would be of interest to evaluate this further in future work.

It will be important to conduct further studies on individual ligand and pan-Hedgehog signalling to monitor their impact on cardiac and renal function. Experimental models exploring acute and chronic myocardial injury and interrogation of existing clinical datasets will be of great value in determining optimal amounts of TNF and Hedgehog pathway modulation for either short and long term indications. Encouragingly, in human patients with rheumatoid arthritis (RA), treatment with biologic agents (>90% of which were TNF antagonists) reduced the incidence of CKD with eGFR<45ml/min by 29% (*78*) whilst TNF antagonists stabilised renal function in patients with RA and CKD compared to other disease modifying drugs (*79*). TNF antagonist treatment also reduced the incidence of total cardiovascular events compared to other agents in RA patients, with protection increasing with longer treatment duration (*80*).

In summary, we found IHH release from renal iPT cells linked TNF release to organ fibrosis. These results suggest that current clinical therapies that target TNF, NFκB and Hedgehog signalling warrant further investigation to assess their efficacy in patients with CKD and fibrosis.

Materials and Methods

Study Design

This study addressed the hypothesis that changes in the renal epithelial phenotype linked aging and inflammation to fibrosis. To answer this a series of controlled laboratory experiments were performed with the primary objective of determining whether distinct subsets of renal epithelia could be identified from murine models of renal injury and aging in vivo, and their contribution to renal fibrosis defined using human cells studied in vitro, in murine models in vivo and by study of previously collected human kidney samples. All studies were conducted in accordance with ARRIVE guidelines (*81*). Based on previous work a two-sided two sample test was used to generate group sizes for all in vivo studies. All studies were performed at the Harvard Medical School, Boston, MA, USA or the University of Edinburgh, UK, with data collection performed at pre-specified endpoints unless limited by animal distress as identified by facility staff and/or veterinary surgeons. No available data was excluded from the analysis. Primary and secondary endpoints were pre-specified. Each mouse represented one experimental unit. Due to the marked protection against post-IRI fibrosis seen in female mice, male mice were used for all IRI experiments. In all experiments, there was randomised allocation to groups. Drug administration and surgical timing was rigorously rotated across all groups. Tissue was collected by two staff members blinded to the treatment groups, using a long established, validated coding system for each animal. Blinded staining and image analysis was undertaken with unblinding only being performed after all data analysis was complete.

Human biopsies and serum analysis

After appropriate ethical approval from Tissue Governance at NHS Lothian, and under the remit of the UK QUOD Consortium supported by NHS Blood and Transplant (REC reference number 20/SS/0105) sections were obtained from renal biopsies from patients tissue with

native renal disease, nephrectomies for renal carcinoma and pre-implantation renal transplants. Assessment for cardiovascular disease was performed based on coded diagnoses in the electronic patient record for at least one of the following conditions: coronary artery disease, ischaemic chest pain, heart attacks, stroke, congestive heart failure and heart rhythm problems as per NIH/NCI criteria (*82*). Human serum samples were analysed using an anti-human IHH sandwich ELISA (LS-F6997, LSBio) according to the manufacturer's instructions.

Statistical Analysis

Data were stored in Excel (Microsoft, USA) and analysed with Prism 9.0 (GraphPad, USA) or R version 4. Multivariable linear regression was performed on R using the finalfit package (1.0.2). All data is expressed as dot plots with bars representing median values. Published human microarray datasets from Rodwell et al.(*30*) were downloaded from the NephroSeq (www.nephroseq.org) online database and linear regression analysis and Kruskal-Wallis tests performed. For all in vivo studies n numbers reflect biological replicates. Depending on the numbers of groups present and the results of normality testing using the Shapiro-Wilk test groups were compared using unpaired Student's unpaired T-test, Mann-Whitney U-test, ANOVA (Tukey's, Dunnett's and Sidak's post-hoc test for multiple comparisons) or Kruskal-Wallis test (with Dunn's multiple comparisons test). All data presented is uploaded and freely available online, or included as supplemental data, alongside normality testing and descriptive statistics including mean values and confidence intervals. P-values < 0.05 denote statistical significance, *$p<0.05$, **$p<0.01$, ***$p<0.005$, ****$p<0.001$.

Supplementary Materials

Materials and Methods

Figs. S1-S14

Tables S1-2

Data file S1.

References

1. A. C. Hearps, G. E. Martin, T. A. Angelovich, W. J. Cheng, A. Maisa, A. L. Landay, A. Jaworowski, S. M. Crowe, Aging is associated with chronic innate immune activation and dysregulation of monocyte phenotype and function. *Aging cell* **11**, 867-875 (2012).
2. G. Santos Morais Junior, D. Ignacio Valenzuela Perez, A. Cecilia Tonet-Furioso, L. Gomes, K. H. Coelho Vilaca, V. Paulo Alves, C. Franco Moraes, O. Toledo Nobrega, Circulating Interleukin-6 (but Not Other Immune Mediators) Associates with Criteria for Fried's Frailty among Very Old Adults. *J Aging Res* **2020**, 6831791 (2020).
3. S. Gencer, B. R. Evans, E. P. C. van der Vorst, Y. Doring, C. Weber, Inflammatory Chemokines in Atherosclerosis. *Cells* **10**, (2021).
4. C. Kurts, U. Panzer, H. J. Anders, A. J. Rees, The immune system and kidney disease: basic concepts and clinical implications. *Nat Rev Immunol* **13**, 738-753 (2013).
5. Y. Sato, M. Yanagita, Immunology of the ageing kidney. *Nat Rev Nephrol* **15**, 625-640 (2019).
6. J. Jankowski, J. Floege, D. Fliser, M. Bohm, N. Marx, Cardiovascular Disease in Chronic Kidney Disease: Pathophysiological Insights and Therapeutic Options. *Circulation* **143**, 1157-1172 (2021).
7. D. J. Nikolic-Paterson, S. Wang, H. Y. Lan, Macrophages promote renal fibrosis through direct and indirect mechanisms. *Kidney international supplements* **4**, 34-38 (2014).
8. K. S. Eardley, C. Kubal, D. Zehnder, M. Quinkler, J. Lepenies, C. O. Savage, A. J. Howie, K. Kaur, M. S. Cooper, D. Adu, P. Cockwell, The role of capillary density, macrophage infiltration and interstitial scarring in the pathogenesis of human chronic kidney disease. *Kidney Int* **74**, 495-504 (2008).
9. P. A. Schytz, P. Blanche, A. B. Nissen, C. Torp-Pedersen, G. H. Gislason, K. E. Nelveg-Kristensen, K. Hommel, N. Carlson, Acute kidney injury and risk of cardiovascular outcomes: A nationwide cohort study. *Nefrologia (Engl Ed)*, (2021).
10. T. A. Ikizler, C. R. Parikh, J. Himmelfarb, V. M. Chinchilli, K. D. Liu, S. G. Coca, A. X. Garg, C. Y. Hsu, E. D. Siew, M. M. Wurfel, L. B. Ware, G. B. Faulkner, T. C. Tan, J. S. Kaufman, P. L. Kimmel, A. S. Go, A.-A. S. Investigators, A prospective cohort study of acute kidney injury and kidney outcomes, cardiovascular events, and death. *Kidney Int* **99**, 456-465 (2021).
11. P. J. Nelson, A. J. Rees, M. D. Griffin, J. Hughes, C. Kurts, J. Duffield, The renal mononuclear phagocytic system. *J Am Soc Nephrol* **23**, 194-203 (2012).
12. F. J. Therrien, M. Agharazii, M. Lebel, R. Lariviere, Neutralization of tumor necrosis factor-alpha reduces renal fibrosis and hypertension in rats with renal failure. *Am J Nephrol* **36**, 151-161 (2012).
13. S. B. Khan, H. T. Cook, G. Bhangal, J. Smith, F. W. Tam, C. D. Pusey, Antibody blockade of TNF-alpha reduces inflammation and scarring in experimental crescentic glomerulonephritis. *Kidney Int* **67**, 1812-1820 (2005).
14. Y. Sato, A. Mii, Y. Hamazaki, H. Fujita, H. Nakata, K. Masuda, S. Nishiyama, S. Shibuya, H. Haga, O. Ogawa, A. Shimizu, S. Narumiya, T. Kaisho, M. Arita, M. Yanagisawa, M. Miyasaka, K. Sharma, N. Minato, H. Kawamoto, M. Yanagita, Heterogeneous fibroblasts underlie age-dependent tertiary lymphoid tissues in the kidney. *JCI Insight* **1**, e87680 (2016).
15. R. Kramann, S. V. Fleig, R. K. Schneider, S. L. Fabian, D. P. DiRocco, O. Maarouf, J. Wongboonsin, Y. Ikeda, D. Heckl, S. L. Chang, H. G. Rennke, S. S. Waikar, B. D.

Humphreys, Pharmacological GLI2 inhibition prevents myofibroblast cell-cycle progression and reduces kidney fibrosis. *J Clin Invest* **125**, 2935-2951 (2015).
16. R. Kramann, C. Goettsch, J. Wongboonsin, H. Iwata, R. K. Schneider, C. Kuppe, N. Kaesler, M. Chang-Panesso, F. G. Machado, S. Gratwohl, K. Madhurima, J. D. Hutcheson, S. Jain, E. Aikawa, B. D. Humphreys, Adventitial MSC-like Cells Are Progenitors of Vascular Smooth Muscle Cells and Drive Vascular Calcification in Chronic Kidney Disease. *Cell stem cell* **19**, 628-642 (2016).
17. R. Kramann, R. K. Schneider, D. P. DiRocco, F. Machado, S. Fleig, P. A. Bondzie, J. M. Henderson, B. L. Ebert, B. D. Humphreys, Perivascular Gli1+ progenitors are key contributors to injury-induced organ fibrosis. *Cell stem cell* **16**, 51-66 (2015).
18. R. Kramann, J. Wongboonsin, M. Chang-Panesso, F. G. Machado, B. D. Humphreys, Gli1(+) Pericyte Loss Induces Capillary Rarefaction and Proximal Tubular Injury. *J Am Soc Nephrol* **28**, 776-784 (2017).
19. R. Kramann, Hedgehog Gli signalling in kidney fibrosis. *Nephrol Dial Transplant* **31**, 1989-1995 (2016).
20. E. Seo, W. Y. Kim, J. Hur, H. Kim, S. A. Nam, A. Choi, Y. M. Kim, S. H. Park, C. Chung, J. Kim, S. Min, S. J. Myung, D. S. Lim, Y. K. Kim, The Hippo-Salvador signaling pathway regulates renal tubulointerstitial fibrosis. *Sci Rep* **6**, 31931 (2016).
21. A. Bera, F. Das, N. Ghosh-Choudhury, M. M. Mariappan, B. S. Kasinath, G. Ghosh Choudhury, Reciprocal regulation of miR-214 and PTEN by high glucose regulates renal glomerular mesangial and proximal tubular epithelial cell hypertrophy and matrix expansion. *American journal of physiology. Cell physiology* **313**, C430-C447 (2017).
22. R. Du, W. Sun, L. Xia, A. Zhao, Y. Yu, L. Zhao, H. Wang, C. Huang, S. Sun, Hypoxia-induced down-regulation of microRNA-34a promotes EMT by targeting the Notch signaling pathway in tubular epithelial cells. *PLoS One* **7**, e30771 (2012).
23. S. Kumar, J. Liu, P. Pang, A. M. Krautzberger, A. Reginensi, H. Akiyama, A. Schedl, B. D. Humphreys, A. P. McMahon, Sox9 Activation Highlights a Cellular Pathway of Renal Repair in the Acutely Injured Mammalian Kidney. *Cell Rep* **12**, 1325-1338 (2015).
24. Y. Kirita, H. Wu, K. Uchimura, P. C. Wilson, B. D. Humphreys, Cell profiling of mouse acute kidney injury reveals conserved cellular responses to injury. *Proc Natl Acad Sci U S A* **117**, 15874-15883 (2020).
25. Y. Muto, P. C. Wilson, N. Ledru, H. Wu, H. Dimke, S. S. Waikar, B. D. Humphreys, Single cell transcriptional and chromatin accessibility profiling redefine cellular heterogeneity in the adult human kidney. *Nature communications* **12**, 2190 (2021).
26. A. B. Sanz, M. D. Sanchez-Nino, A. M. Ramos, J. A. Moreno, B. Santamaria, M. Ruiz-Ortega, J. Egido, A. Ortiz, NF-kappaB in renal inflammation. *J Am Soc Nephrol* **21**, 1254-1262 (2010).
27. L. Marko, E. Vigolo, C. Hinze, J. K. Park, G. Roel, A. Balogh, M. Choi, A. Wubken, J. Cording, I. E. Blasig, F. C. Luft, C. Scheidereit, K. M. Schmidt-Ott, R. Schmidt-Ullrich, D. N. Muller, Tubular Epithelial NF-kappaB Activity Regulates Ischemic AKI. *J Am Soc Nephrol* **27**, 2658-2669 (2016).
28. C. Tabula Muris, A single-cell transcriptomic atlas characterizes ageing tissues in the mouse. *Nature* **583**, 590-595 (2020).
29. J. I. Jun, L. F. Lau, Taking aim at the extracellular matrix: CCN proteins as emerging therapeutic targets. *Nat Rev Drug Discov* **10**, 945-963 (2011).
30. G. E. Rodwell, R. Sonu, J. M. Zahn, J. Lund, J. Wilhelmy, L. Wang, W. Xiao, M. Mindrinos, E. Crane, E. Segal, B. D. Myers, J. D. Brooks, R. W. Davis, J. Higgins, A.

B. Owen, S. K. Kim, A transcriptional profile of aging in the human kidney. *PLoS biology* **2**, e427 (2004).
31. M. Perrot-Applanat, S. Vacher, A. Toullec, I. Pelaez, G. Velasco, F. Cormier, S. Saad Hel, R. Lidereau, V. Baud, I. Bieche, Similar NF-kappaB gene signatures in TNF-alpha treated human endothelial cells and breast tumor biopsies. *PLoS One* **6**, e21589 (2011).
32. S. Abel, C. Hundhausen, R. Mentlein, A. Schulte, T. A. Berkhout, N. Broadway, D. Hartmann, R. Sedlacek, S. Dietrich, B. Muetze, B. Schuster, K. J. Kallen, P. Saftig, S. Rose-John, A. Ludwig, The transmembrane CXC-chemokine ligand 16 is induced by IFN-gamma and TNF-alpha and shed by the activity of the disintegrin-like metalloproteinase ADAM10. *J Immunol* **172**, 6362-6372 (2004).
33. P. Gong, A. Canaan, B. Wang, J. Leventhal, A. Snyder, V. Nair, C. D. Cohen, M. Kretzler, V. D'Agati, S. Weissman, M. J. Ross, The ubiquitin-like protein FAT10 mediates NF-kappaB activation. *J Am Soc Nephrol* **21**, 316-326 (2010).
34. E. Mehaffey, D. S. A. Majid, Tumor necrosis factor-alpha, kidney function, and hypertension. *Am J Physiol Renal Physiol* **313**, F1005-F1008 (2017).
35. B. Cvek, Z. Dvorak, The ubiquitin-proteasome system (UPS) and the mechanism of action of bortezomib. *Current pharmaceutical design* **17**, 1483-1499 (2011).
36. A. Yamakawa, H. Hojo, U. Chung, S. Ohba, IDENTIFICATION OF A CHONDROCYTE-SPECIFIC INDIAN HEDGEHOG ENHANCER AND SOX9-MEDIATED MECHANISMS OF THE ENHANCER ACTIVATION. *Osteoarthritis and Cartilage* **16**, S10-S59 (2018).
37. M. Edeling, G. Ragi, S. Huang, H. Pavenstadt, K. Susztak, Developmental signalling pathways in renal fibrosis: the roles of Notch, Wnt and Hedgehog. *Nat Rev Nephrol* **12**, 426-439 (2016).
38. D. Zhou, Y. Li, L. Zhou, R. J. Tan, L. Xiao, M. Liang, F. F. Hou, Y. Liu, Sonic hedgehog is a novel tubule-derived growth factor for interstitial fibroblasts after kidney injury. *J Am Soc Nephrol* **25**, 2187-2200 (2014).
39. B. R. Conway, E. D. O'Sullivan, C. Cairns, J. O'Sullivan, D. J. Simpson, A. Salzano, K. Connor, P. Ding, D. Humphries, K. Stewart, O. Teenan, R. Pius, N. C. Henderson, C. Benezech, P. Ramachandran, D. Ferenbach, J. Hughes, T. Chandra, L. Denby, Kidney Single-Cell Atlas Reveals Myeloid Heterogeneity in Progression and Regression of Kidney Disease. *J Am Soc Nephrol* **31**, 2833-2854 (2020).
40. A. Horn, K. Palumbo, C. Cordazzo, C. Dees, A. Akhmetshina, M. Tomcik, P. Zerr, J. Avouac, J. Gusinde, J. Zwerina, H. Roudaut, E. Traiffort, M. Ruat, O. Distler, G. Schett, J. H. Distler, Hedgehog signaling controls fibroblast activation and tissue fibrosis in systemic sclerosis. *Arthritis Rheum* **64**, 2724-2733 (2012).
41. J. Espana-Agusti, X. Zou, K. Wong, B. Fu, F. Yang, D. A. Tuveson, D. J. Adams, A. Matakidou, Generation and Characterisation of a Pax8-CreERT2 Transgenic Line and a Slc22a6-CreERT2 Knock-In Line for Inducible and Specific Genetic Manipulation of Renal Tubular Epithelial Cells. *PLoS One* **11**, e0148055 (2016).
42. B. St-Jacques, M. Hammerschmidt, A. P. McMahon, Indian hedgehog signaling regulates proliferation and differentiation of chondrocytes and is essential for bone formation. *Genes & development* **13**, 2072-2086 (1999).
43. M. Lenarczyk, E. C. Laiakis, D. L. Mattson, B. D. Johnson, A. Kronenberg, P. E. North, R. Komorowski, M. Mader, J. E. Baker, Irradiation of the kidneys causes pathologic remodeling in the nontargeted heart: A role for the immune system. *FASEB Bioadv* **2**, 705-719 (2020).
44. L. Arcari, J. Engel, T. Freiwald, H. Zhou, H. Zainal, M. Gawor, S. Buettner, H. Geiger, I. Hauser, E. Nagel, V. O. Puntmann, Cardiac biomarkers in chronic kidney

disease are independently associated with myocardial edema and diffuse fibrosis by cardiovascular magnetic resonance. *J Cardiovasc Magn Reson* **23**, 71 (2021).
45. Y. Yoshida, N. Matsunaga, T. Nakao, K. Hamamura, H. Kondo, T. Ide, H. Tsutsui, A. Tsuruta, M. Kurogi, M. Nakaya, H. Kurose, S. Koyanagi, S. Ohdo, Alteration of circadian machinery in monocytes underlies chronic kidney disease-associated cardiac inflammation and fibrosis. *Nature communications* **12**, 2783 (2021).
46. D. M. Charytan, R. Padera, A. M. Helfand, M. Zeisberg, X. Xu, X. Liu, J. Himmelfarb, A. Cinelli, R. Kalluri, E. M. Zeisberg, Increased concentration of circulating angiogenesis and nitric oxide inhibitors induces endothelial to mesenchymal transition and myocardial fibrosis in patients with chronic kidney disease. *International journal of cardiology* **176**, 99-109 (2014).
47. F. C. Yin, H. A. Spurgeon, K. Rakusan, M. L. Weisfeldt, E. G. Lakatta, Use of tibial length to quantify cardiac hypertrophy: application in the aging rat. *The American journal of physiology* **243**, H941-947 (1982).
48. H. Kawagishi, J. Xiong, Rovira, II, H. Pan, Y. Yan, B. K. Fleischmann, M. Yamada, T. Finkel, Sonic hedgehog signaling regulates the mammalian cardiac regenerative response. *Journal of molecular and cellular cardiology* **123**, 180-184 (2018).
49. K. F. Kusano, R. Pola, T. Murayama, C. Curry, A. Kawamoto, A. Iwakura, S. Shintani, M. Ii, J. Asai, T. Tkebuchava, T. Thorne, H. Takenaka, R. Aikawa, D. Goukassian, P. von Samson, H. Hamada, Y. S. Yoon, M. Silver, E. Eaton, H. Ma, L. Heyd, M. Kearney, W. Munger, J. A. Porter, R. Kishore, D. W. Losordo, Sonic hedgehog myocardial gene therapy: tissue repair through transient reconstitution of embryonic signaling. *Nature medicine* **11**, 1197-1204 (2005).
50. K. Song, Y. Qing, Q. Guo, E. K. Peden, C. Chen, W. E. Mitch, L. Truong, J. Cheng, PDGFRA in vascular adventitial MSCs promotes neointima formation in arteriovenous fistula in chronic kidney disease. *JCI Insight* **5**, (2020).
51. G. B. D. C. K. D. Collaboration, Global, regional, and national burden of chronic kidney disease, 1990-2017: a systematic analysis for the Global Burden of Disease Study 2017. *Lancet* **395**, 709-733 (2020).
52. J. Coresh, E. Selvin, L. A. Stevens, J. Manzi, J. W. Kusek, P. Eggers, F. Van Lente, A. S. Levey, Prevalence of chronic kidney disease in the United States. *JAMA* **298**, 2038-2047 (2007).
53. L. M. S. Gerhardt, J. Liu, K. Koppitch, P. E. Cippa, A. P. McMahon, Single-nuclear transcriptomics reveals diversity of proximal tubule cell states in a dynamic response to acute kidney injury. *Proc Natl Acad Sci U S A* **118**, (2021).
54. S. Ide, Y. Kobayashi, K. Ide, S. A. Strausser, K. Abe, S. Herbek, L. L. O'Brien, S. D. Crowley, L. Barisoni, A. Tata, P. R. Tata, T. Souma, Ferroptotic stress promotes the accumulation of pro-inflammatory proximal tubular cells in maladaptive renal repair. *Elife* **10**, (2021).
55. Y. A. Lu, C. T. Liao, R. Raybould, B. Talabani, I. Grigorieva, B. Szomolay, T. Bowen, R. Andrews, P. R. Taylor, D. Fraser, Single-Nucleus RNA Sequencing Identifies New Classes of Proximal Tubular Epithelial Cells in Kidney Fibrosis. *J Am Soc Nephrol* **32**, 2501-2516 (2021).
56. H. Ding, D. Zhou, S. Hao, L. Zhou, W. He, J. Nie, F. F. Hou, Y. Liu, Sonic hedgehog signaling mediates epithelial-mesenchymal communication and promotes renal fibrosis. *J Am Soc Nephrol* **23**, 801-813 (2012).
57. Y. Jung, K. D. Brown, R. P. Witek, A. Omenetti, L. Yang, M. Vandongen, R. J. Milton, I. N. Hines, R. A. Rippe, L. Spahr, L. Rubbia-Brandt, A. M. Diehl, Accumulation of hedgehog-responsive progenitors parallels alcoholic liver disease severity in mice and humans. *Gastroenterology* **134**, 1532-1543 (2008).

58. A. Omenetti, A. Porrello, Y. Jung, L. Yang, Y. Popov, S. S. Choi, R. P. Witek, G. Alpini, J. Venter, H. M. Vandongen, W. K. Syn, G. S. Baroni, A. Benedetti, D. Schuppan, A. M. Diehl, Hedgehog signaling regulates epithelial-mesenchymal transition during biliary fibrosis in rodents and humans. *J Clin Invest* **118**, 3331-3342 (2008).
59. Y. Jung, S. J. McCall, Y. X. Li, A. M. Diehl, Bile ductules and stromal cells express hedgehog ligands and/or hedgehog target genes in primary biliary cirrhosis. *Hepatology* **45**, 1091-1096 (2007).
60. A. Kothandapani, C. R. Jefcoate, J. S. Jorgensen, Cholesterol Contributes to Male Sex Differentiation Through Its Developmental Role in Androgen Synthesis and Hedgehog Signaling. *Endocrinology* **162**, (2021).
61. W. T. Lv, D. H. Du, R. J. Gao, C. W. Yu, Y. Jia, Z. F. Jia, C. J. Wang, Regulation of Hedgehog signaling Offers A Novel Perspective for Bone Homeostasis Disorder Treatment. *Int J Mol Sci* **20**, (2019).
62. T. R. Hartman, D. Zinshteyn, H. K. Schofield, E. Nicolas, A. Okada, A. M. O'Reilly, Drosophila Boi limits Hedgehog levels to suppress follicle stem cell proliferation. *J Cell Biol* **191**, 943-952 (2010).
63. I. H. Jung, D. E. Jung, Y. N. Park, S. Y. Song, S. W. Park, Aberrant Hedgehog ligands induce progressive pancreatic fibrosis by paracrine activation of myofibroblasts and ductular cells in transgenic zebrafish. *PLoS One* **6**, e27941 (2011).
64. H. Y. Kim, H. K. Cho, S. P. Hong, J. Cheong, Hepatitis B virus X protein stimulates the Hedgehog-Gli activation through protein stabilization and nuclear localization of Gli1 in liver cancer cells. *Cancer letters* **309**, 176-184 (2011).
65. G. M. Philips, I. S. Chan, M. Swiderska, V. T. Schroder, C. Guy, G. F. Karaca, C. Moylan, T. Venkatraman, S. Feuerlein, W. K. Syn, Y. Jung, R. P. Witek, S. Choi, G. A. Michelotti, F. Rangwala, E. Merkle, C. Lascola, A. M. Diehl, Hedgehog signaling antagonist promotes regression of both liver fibrosis and hepatocellular carcinoma in a murine model of primary liver cancer. *PLoS One* **6**, e23943 (2011).
66. M. Dunaeva, J. Waltenberger, Hh signaling in regeneration of the ischemic heart. *Cell Mol Life Sci* **74**, 3481-3490 (2017).
67. B. Ochoa, W. K. Syn, I. Delgado, G. F. Karaca, Y. Jung, J. Wang, A. M. Zubiaga, O. Fresnedo, A. Omenetti, M. Zdanowicz, S. S. Choi, A. M. Diehl, Hedgehog signaling is critical for normal liver regeneration after partial hepatectomy in mice. *Hepatology* **51**, 1712-1723 (2010).
68. S. S. Choi, A. Omenetti, R. P. Witek, C. A. Moylan, W. K. Syn, Y. Jung, L. Yang, D. L. Sudan, J. K. Sicklick, G. A. Michelotti, M. Rojkind, A. M. Diehl, Hedgehog pathway activation and epithelial-to-mesenchymal transitions during myofibroblastic transformation of rat hepatic cells in culture and cirrhosis. *American journal of physiology. Gastrointestinal and liver physiology* **297**, G1093-1106 (2009).
69. M. F. Bijlsma, P. J. Leenders, B. J. Janssen, M. P. Peppelenbosch, H. Ten Cate, C. A. Spek, Endogenous hedgehog expression contributes to myocardial ischemia-reperfusion-induced injury. *Experimental biology and medicine* **233**, 989-996 (2008).
70. J. Zhang, M. B. Patel, R. Griffiths, A. Mao, Y. S. Song, N. S. Karlovich, M. A. Sparks, H. Jin, M. Wu, E. E. Lin, S. D. Crowley, Tumor necrosis factor-alpha produced in the kidney contributes to angiotensin II-dependent hypertension. *Hypertension* **64**, 1275-1281 (2014).
71. D. Daoussis, A. Filippopoulou, S. N. Liossis, C. Sirinian, K. Klavdianou, P. Bouris, N. K. Karamanos, A. P. Andonopoulos, Anti-TNFalpha treatment decreases the previously increased serum Indian Hedgehog levels in patients with ankylosing

spondylitis and affects the expression of functional Hedgehog pathway target genes. *Semin Arthritis Rheum* **44**, 646-651 (2015).
72. Z. Dai, T. Aoki, Y. Fukumoto, H. Shimokawa, Coronary perivascular fibrosis is associated with impairment of coronary blood flow in patients with non-ischemic heart failure. *Journal of cardiology* **60**, 416-421 (2012).
73. G. Romero-Gonzalez, A. Gonzalez, B. Lopez, S. Ravassa, J. Diez, Heart failure in chronic kidney disease: the emerging role of myocardial fibrosis. *Nephrol Dial Transplant*, (2020).
74. A. Biernacka, N. G. Frangogiannis, Aging and Cardiac Fibrosis. *Aging and disease* **2**, 158-173 (2011).
75. K. Ytrehus, J. S. Hulot, C. Perrino, G. G. Schiattarella, R. Madonna, Perivascular fibrosis and the microvasculature of the heart. Still hidden secrets of pathophysiology? *Vascular pharmacology*, (2018).
76. X. Liu, J. Miao, C. Wang, S. Zhou, S. Chen, Q. Ren, X. Hong, Y. Wang, F. F. Hou, L. Zhou, Y. Liu, Tubule-derived exosomes play a central role in fibroblast activation and kidney fibrosis. *Kidney Int* **97**, 1181-1195 (2020).
77. A. Bhat, A. Sharma, A. C. Bharti, Upstream Hedgehog signaling components are exported in exosomes of cervical cancer cell lines. *Nanomedicine (Lond)* **13**, 2127-2138 (2018).
78. K. Sumida, M. Z. Molnar, P. K. Potukuchi, F. Hassan, F. Thomas, K. Yamagata, K. Kalantar-Zadeh, C. P. Kovesdy, Treatment of rheumatoid arthritis with biologic agents lowers the risk of incident chronic kidney disease. *Kidney Int* **93**, 1207-1216 (2018).
79. H. W. Kim, C. K. Lee, H. S. Cha, J. Y. Choe, E. J. Park, J. Kim, Effect of anti-tumor necrosis factor alpha treatment of rheumatoid arthritis and chronic kidney disease. *Rheumatol Int* **35**, 727-734 (2015).
80. M. Nurmohamed, Y. Bao, J. Signorovitch, A. Trahey, P. Mulani, D. E. Furst, Longer durations of antitumour necrosis factor treatment are associated with reduced risk of cardiovascular events in patients with rheumatoid arthritis. *RMD Open* **1**, e000080 (2015).
81. C. Kilkenny, W. J. Browne, I. C. Cuthill, M. Emerson, D. G. Altman, Improving bioscience research reporting: the ARRIVE guidelines for reporting animal research. *PLoS biology* **8**, e1000412 (2010).
82. in *NCI Dictionary*. vol. 2021, pp. Web dictionary.
83. K. Araki, M. Araki, J. Miyazaki, P. Vassalli, Site-specific recombination of a transgene in fertilized eggs by transient expression of Cre recombinase. Proc Natl Acad Sci U S A 92, 160-164 (1995).
84. D. A. Ferenbach, N. C. Nkejabega, J. McKay, A. K. Choudhary, M. A. Vernon, M. F. Beesley, S. Clay, B. C. Conway, L. P. Marson, D. C. Kluth, J. Hughes, The induction of macrophage hemeoxygenase-1 is protective during acute kidney injury in aging mice. Kidney Int 79, 966-976 (2011).
85. Y. Wang, S. E. Thatcher, L. A. Cassis, Measuring Blood Pressure Using a Noninvasive Tail Cuff Method in Mice. Methods Mol Biol 1614, 69-73 (2017).
86. T. Kipari, J. F. Cailhier, D. Ferenbach, S. Watson, K. Houlberg, D. Walbaum, S. Clay, J. Savill, J. Hughes, Nitric oxide is an important mediator of renal tubular epithelial cell death in vitro and in murine experimental hydronephrosis. Am J Pathol 169, 388-399 (2006).
87. M. L. Lindsey, Z. Kassiri, J. A. I. Virag, L. E. de Castro Bras, M. Scherrer-Crosbie, Guidelines for measuring cardiac physiology in mice. American journal of physiology. Heart and circulatory physiology 314, H733-H752 (2018).

88. F. Wang, J. Flanagan, N. Su, L. C. Wang, S. Bui, A. Nielson, X. Wu, H. T. Vo, X. J. Ma, Y. Luo, RNAscope: a novel in situ RNA analysis platform for formalin-fixed, paraffin- embedded tissues. J Mol Diagn 14, 22-29 (2012).
89. P. Bankhead, M. B. Loughrey, J. A. Fernandez, Y. Dombrowski, D. G. McArt, P. D. Dunne, S. McQuaid, R. T. Gray, L. J. Murray, H. G. Coleman, J. A. James, M. Salto-Tellez, P. W. Hamilton, QuPath: Open source software for digital pathology image analysis. Sci Rep 7, 16878 (2017).
90. A. Dobin, C. A. Davis, F. Schlesinger, J. Drenkow, C. Zaleski, S. Jha, P. Batut, M. Chaisson, T. R. Gingeras, STAR: ultrafast universal RNA-seq aligner. Bioinformatics 29, 15- 21 (2013).
91. A. Butler, P. Hoffman, P. Smibert, E. Papalexi, R. Satija, Integrating single-cell transcriptomic data across different conditions, technologies, and species. Nature biotechnology 36, 411-420 (2018).
92. T. Ilicic, J. K. Kim, A. A. Kolodziejczyk, F. O. Bagger, D. J. McCarthy, J. C. Marioni, S. A. Teichmann, Classification of low quality cells from single-cell RNA-seq data. Genome biology 17, 29 (2016).

Acknowledgements

The authors gratefully acknowledge the staff from the Queen's Medical Research Institute and the Bioresearch and Veterinary services facility at Edinburgh University for their expertise & assistance in this work and the assistance of Professor Bob Hill in obtaining Ihh fl/fl mice. The authors thank the UK QUOD consortium for the clinical samples analyzed in this study. The authors also thank Professor Stuart Forbes, Dr Prakash Ramachandran and Professor Sir John Savill for their proof-reading and advice on this manuscript.

Funding

EOS was supported by a Clinical Training fellowship from Kidney Research UK [TF_006_20161125]. KJM is supported by a Senior Fellowship from Kidney Research UK Fellowship [CSO_PDF/2018/1]. DB and MD are supported by MRC Clinical Training Fellowships. KG was funded by the Chief Scientist Office Scotland [CSO TCS/18/15], Kidney Research UK and the MRC. AL is supported by the Chief Scientist Office Scotland with a NRS Career Researcher Fellowship. JW is supported by the Austrian Science Fund (P30373). BRC was supported by a Kidney Research UK project grant [RP30/2015]. LD is supported by a Senior Fellowship from Kidney Research UK [SF_001_20181122] and funding from British Heart Foundation Ph.D. studentship FS/15/63/32033. AM is supported by the MRC. KK is supported by the MRC (MR/W000148/1). LB is supported by Cancer Research UK (C52499/A27948). NCH is supported by a Wellcome Trust Senior Research Fellowship in Clinical Science (ref. 219542/Z/19/Z). RC is supported by the Wellcome Trust (108906/Z/15/Z). JVB is supported by grants from the National Institutes of Health/National Institute of Diabetes and Digestive and Kidney Diseases (UH3 TR002155 and R37 DK39773, and RO1 DK072381). DAF was supported by an Intermediate Clinical Fellowship

from the Wellcome Trust [100171/Z/12/Z] and a Senior Clinical Fellowship from the MRC [MR/X006735/1].

Author contributions

EDO performed experiments and bioinformatic analysis, analysed results and co-wrote the manuscript. KJM performed experiments, analysed results and co-wrote the manuscript. CX performed experiments and analysed results. DB performed experiments and analysed results CC performed experiments and analysed results. MHD performed experiments and analysed results. RC performed experiments and analysed results. KPM performed experiments and analysed results. SHW performed experiments and analysed results. AW performed experiments and analysed results. KMG performed experiments and analysed results. SJ performed analysis. SL collected tissues for analysis. AL collected tissues for analysis. JW performed bioinformatic analysis. MW performed bioinformatic analysis. MR performed analysis. SF performed analysis. AP performed bioinformatic analysis. SGK performed analysis. AM assisted with experimental design and resources. LB assisted with experimental design, resources, funding and writing of the manuscript. NCH assisted with experimental design. KK provided tuition and support with bioinformatic analysis. TC provided tuition and support with bioinformatic analysis. BRC assisted with experimental design and writing of the manuscript. JH assisted with experimental design and writing of the manuscript. LD assisted with experimental design, resources, funding and writing of the manuscript. JVB hosted initial studies, assisted with experimental design and writing of the manuscript. DAF provided funding, designed the studies, analysed results and edited the manuscript

Competing Interests

JVB is an advisor with equity in Oisin Biotherapeutics, an advisor to Serepta, Stugen and Sareptou, and has been a consultant to Janssen and AstraZeneca. JVB is an inventor on KIM-1 patents that are assigned to MassGeneralBrigham. DAF has received research funding from Argenx, undertaken consultancy work for Rejuvenon Life Sciences and is on the scientific advisory board of Dorian Therapeutics. All other authors have no competing interests.

Data and Materials Availability

All data has been included in the Supplementary Materials of this paper, or has been deposited in the National Center for Biotechnology Information Gene Expression Omnibus database (accession # GSE178109). Data from Tabula Muris Senis can be found at https://tabula-muris-senis.ds.czbiohub.org/.

Figure Captions:

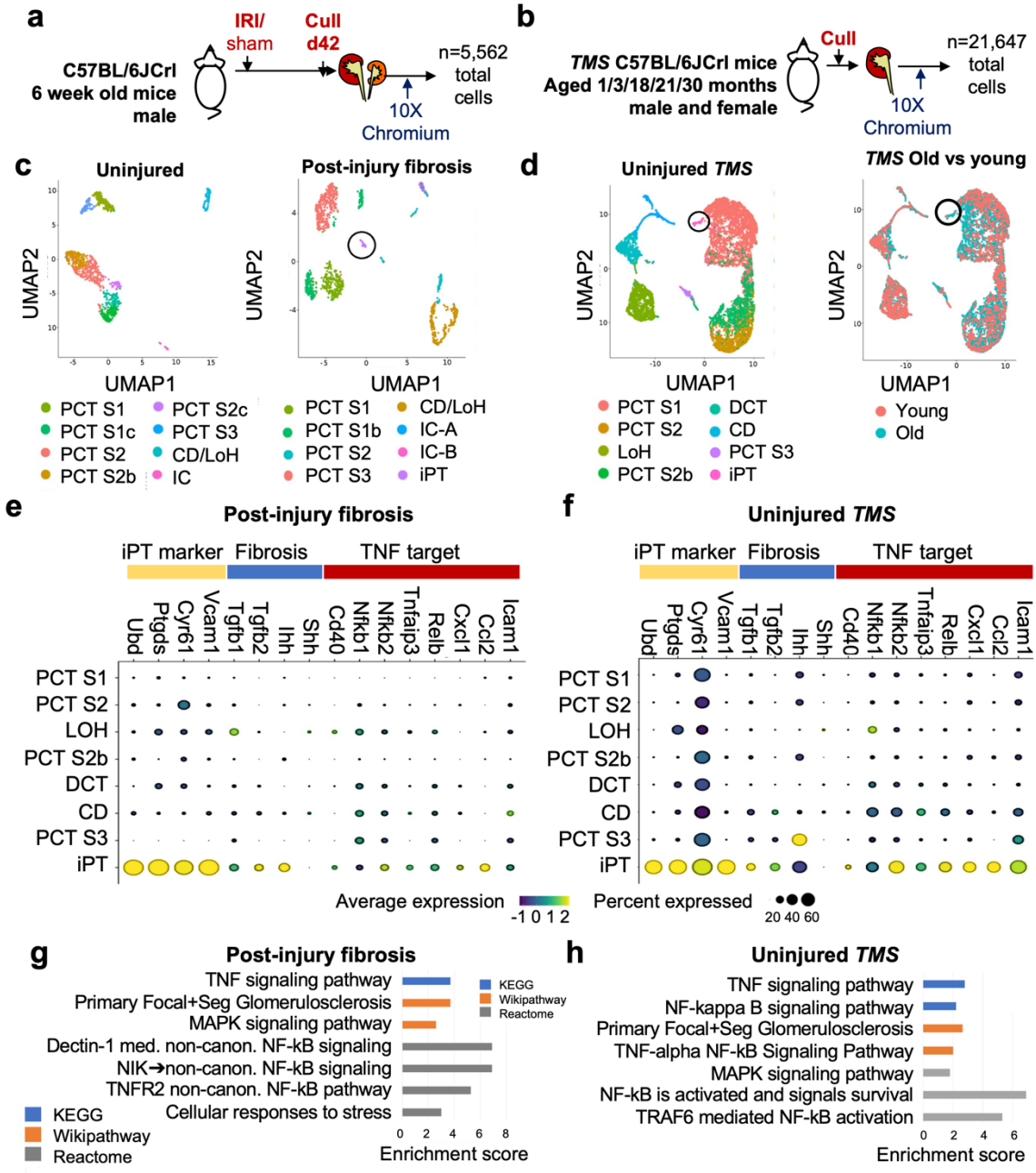

Figure 1. Identification of inflammatory proximal tubular cells in injured and aging mouse kidneys. (A-B) Schema of single cell analyses of renal epithelia performed in young murine kidneys with fibrosis 42 days post ischemia reperfusion injury (**A,** n=3/group) and healthy young and aged kidneys from the *Tabula Muris Senis* (*TMS*) dataset (**B,** total n=14, n=2-4/timepoint). (C-D, PCT – proximal convoluted tubule, LoH – loop of Henle, CD – collecting duct, IC – intercalated cell, iPT – inflammatory proximal tubule). Analysis using

Seurat demonstrated additional clusters absent from healthy young epithelia but present in previously injured kidneys (**C**) and aged kidneys (**D)** indicated by black circles on each Uniform Manifold Approximation and Projection (UMAP) plot. (E-F) A subset of cell identity, fibrosis and TNF signaling related genes are shown for injured kidneys (**E**), and aged kidneys (**F**). Over representation analysis (ORA) of the inflammatory proximal tubule cluster is shown in previously injured kidneys (**G**) and aged kidneys (**H**). Blue bars indicate analyses from KEGG enrichment, orange indicates Wikipathway enrichment and grey indicates Reactome enrichment. False discovery rate <0.05.

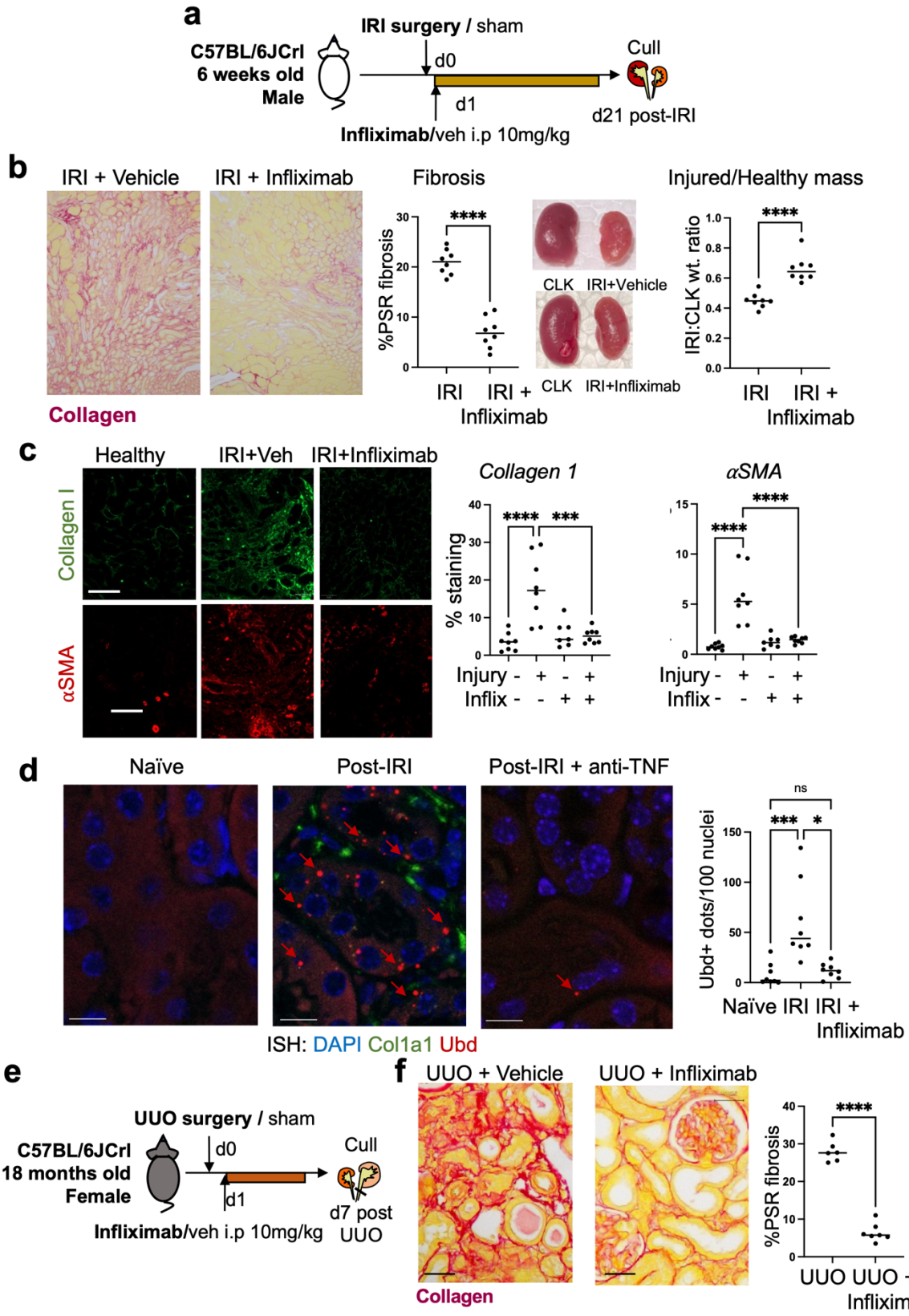

Figure 2. Profibrotic inflammatory proximal tubular cells increase in response to TNF in mice in vivo. **(A)** Schema of TNF inhibition studies using Infliximab (10mg/kg) after

unilateral IRI (n=8/group). **(B)** %Picrosirius Red (PSR) staining for renal fibrosis after ischaemic injury, including the ratio of weights of the injured kidney relative to the contralateral uninjured kidney (IRI:CLK weight ratio:n=8/group, unpaired t-test). **(C)** Immunofluorescence staining and quantification of Collagen I deposition (green) and αSMA+ myofibroblast expansion (red) after uIRI (n=7-8/group, one way ANOVA with Tukey's test) **(D)** ISH and quantification of Ubd+ iPT cells in uIRI kidney (Blue=DAPI, Red=Ubd, Green=Col1a1, n=8/group, Kruskal-Wallis test). **I** Schema of Infliximab studies with unilateral ureteric obstruction in aged mice (n=6-7/group). **(F)** PSR staining and quantification of fibrosis after UUO in aged mice (n=6-7/group, unpaired t-test). Scale bars: 100microns (B-C), 50microns (E), 10microns (D). Each image is representative of image acquisition and analysis performed from all experimental subjects. *p<0.05, **p<0.01, ***p<0.001, ****p<0.0001.

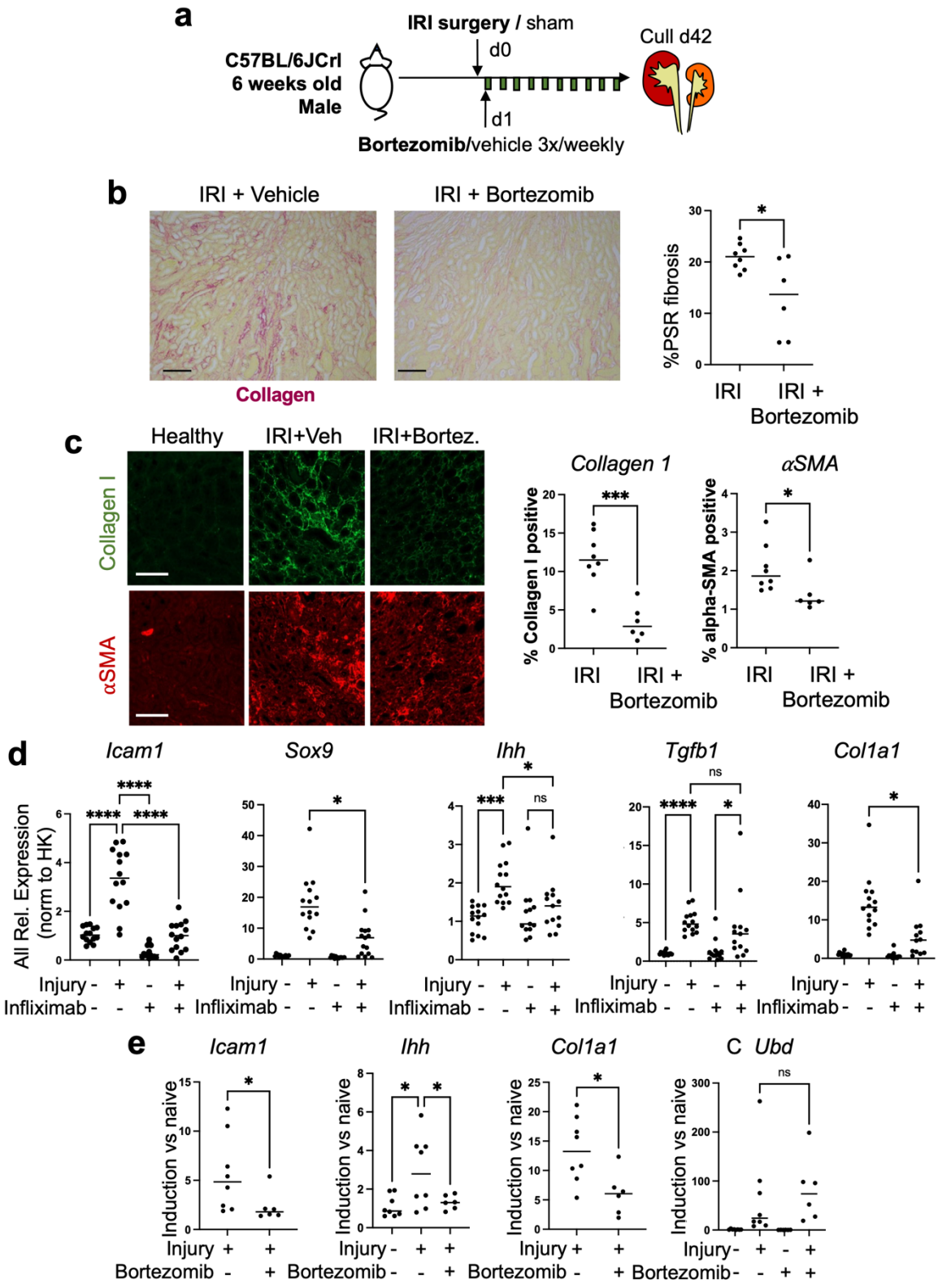

Figure 3. Profibrotic inflammatory proximal tubular activation is inhibited by blockade of NFκB signalling. **(G)** Schematic of Bortezomib studies after uIRI in the murine kidney **(H)** PSR staining of kidney tissue after IRI ± Bortezomib treatment (n=6-8/group, unpaired t-test)

(I) Immunofluorescence staining and quantification of Collagen I deposition and αSMA+ myofibroblast expansion after uIRI (n=6-8/group, unpaired t and Mann-Whitney tests). **(J)** mRNA expression of *Icam1*, *Sox9, Ihh, Tgfb1* and *Col1a1* after injury, normalized to housekeeping genes and expressed relative to naïve, vehicle treated kidneys (n=12-14/group, ANOVA with Tukey's test or Kruskal-Wallis test). **(K)** mRNA expression of *Icam1*, *Ihh*, *Col1a1* and *Ubd* after injury, normalized to housekeeping genes and expressed relative to naïve, vehicle treated kidneys (n=6-8/group, ANOVA, Kruskal-Wallis and unpaired t-tests). Scale bars: 100microns (A). Each image is representative of image acquisition and analysis performed from all experimental subjects. *p<0.05, **p<0.01, ***p<0.001, ****p<0.0001.

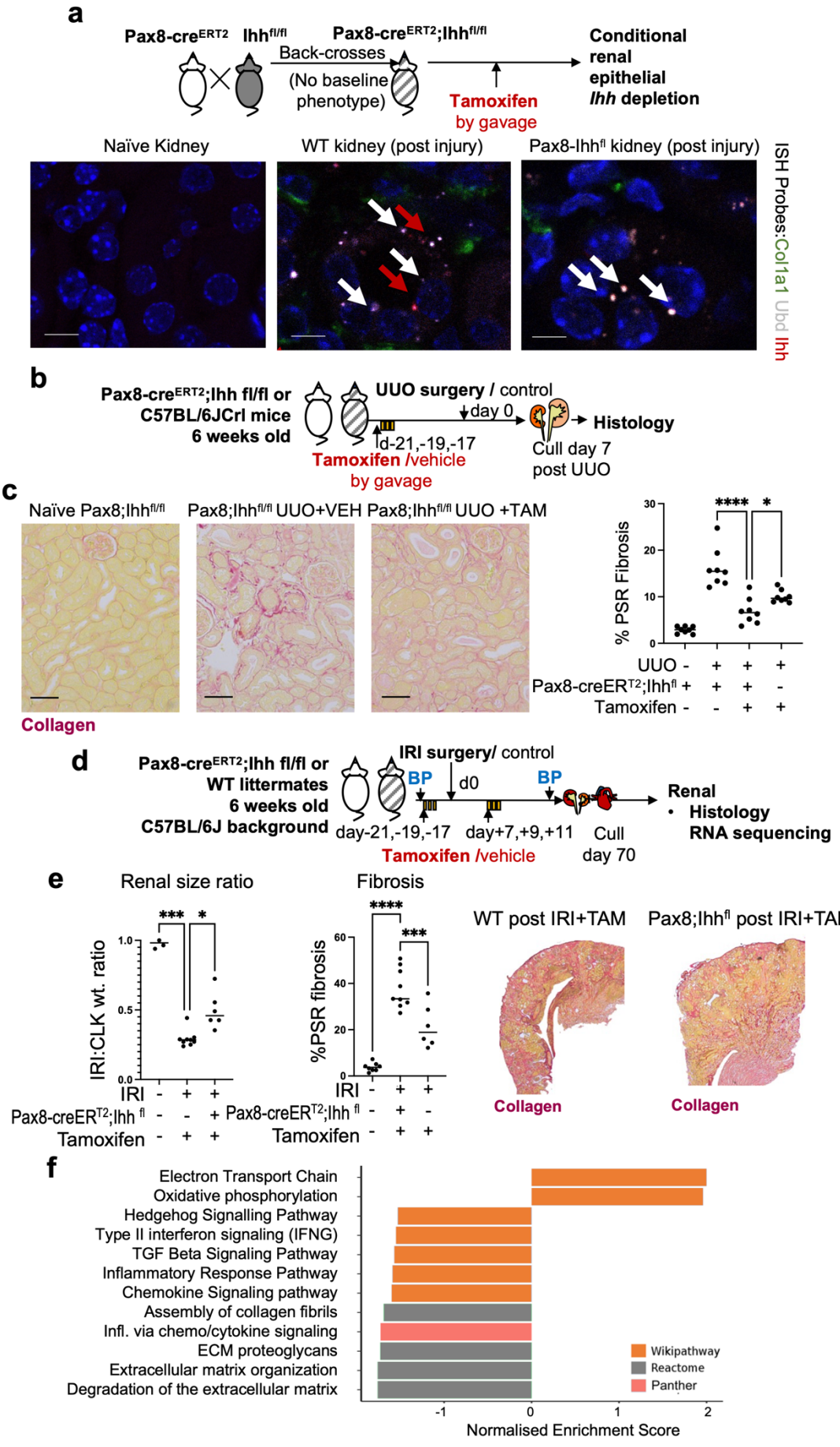
a
Pax8-creERT2
Ihhfl/fl
Back-crosses
(No baseline phenotype)
Pax8-creERT2;Ihhfl/fl
Tamoxifen by gavage
Conditional renal epithelial Ihh depletion
Naïve Kidney
WT kidney (post injury)
Pax8-Ihhfl kidney (post injury)
ISH Probes:Col1a1 Ubd Ihh
b
Pax8-creERT2;Ihh fl/fl or C57BL/6JCrl mice 6 weeks old
UUO surgery / control
day 0
d-21,-19,-17
Tamoxifen /vehicle by gavage
Histology
Cull day 7 post UUO
c
Naïve Pax8;Ihhfl/fl
Pax8;Ihhfl/fl UUO+VEH
Pax8;Ihhfl/fl UUO +TAM
Collagen
% PSR Fibrosis
****
*
UUO
Pax8-creERT2;Ihhfl
Tamoxifen
d
Pax8-creERT2;Ihh fl/fl or WT littermates 6 weeks old C57BL/6J background
IRI surgery/ control
BP
d0
BP
day-21,-19,-17
Tamoxifen /vehicle
day+7,+9,+11
Cull day 70
Renal
• Histology
RNA sequencing
e
Renal size ratio
IRI:CLK wt. ratio
***
*
IRI
Pax8-creERT2;Ihh fl
Tamoxifen
Fibrosis
%PSR fibrosis
****
***
WT post IRI+TAM
Pax8;Ihhfl post IRI+TAM
Collagen
Collagen
f
Electron Transport Chain
Oxidative phosphorylation
Hedgehog Signalling Pathway
Type II interferon signaling (IFNG)
TGF Beta Signaling Pathway
Inflammatory Response Pathway
Chemokine Signaling pathway
Assembly of collagen fibrils
Infl. via chemo/cytokine signaling
ECM proteoglycans
Extracellular matrix organization
Degradation of the extracellular matrix
Wikipathway
Reactome
Panther
Normalised Enrichment Score

Figure 4. Indian Hedgehog is associated with renal fibrosis in mice and humans. (A) Schema of breeding strategy used to generate Pax8-cre^{ERT2}; Ihh$^{fl/fl}$ mice and confocal images of *Col1a1*, *Ubd* and *Ihh* transcripts in healthy and injured kidneys from wild-type (WT) and Pax8-cre^{ERT2}; Ihh$^{fl/fl}$ transgenic (TG) mice. White arrows: *Ubd* transcripts. Red arrows: *Ihh* transcripts. Blue staining represents nuclei (DAPI). **(B)** Schema of experiments testing the Ihh deletion in unilateral ureteric obstruction in mice. **(C)** Picrosirius Red staining and %PSR in Pax8-cre^{ERT2}; Ihh$^{fl/fl}$ mice after UUO (n=8/group, ANOVA with Sidak's test). **(D)** Schematic of experiments using Pax8-cre^{ERT2}; Ihh$^{fl/fl}$ mice to test the role of *Ihh* during renal uIRI. **(E)** Quantification of kidney mass and fibrosis (%PSR) in Pax8-cre^{ERT2}; Ihh$^{fl/fl}$ mice with representative images (right) post uIRI (n=4-9/group, ANOVA with Tukey's test, and Kruskal-Wallis tests) **(F)** Over-representation analysis illustrates up and downregulated pathways in *Ihh* deleted kidneys post-uIRI. Orange = Wikipathway, Grey = Reactome, Pink = Panther. Scale bars: 100microns (C), 10 microns (A): Each image is representative of image acquisition and analysis performed from all experimental subjects. *p<0.05, **p<0.01, ***p<0.001, ****p<0.0001.

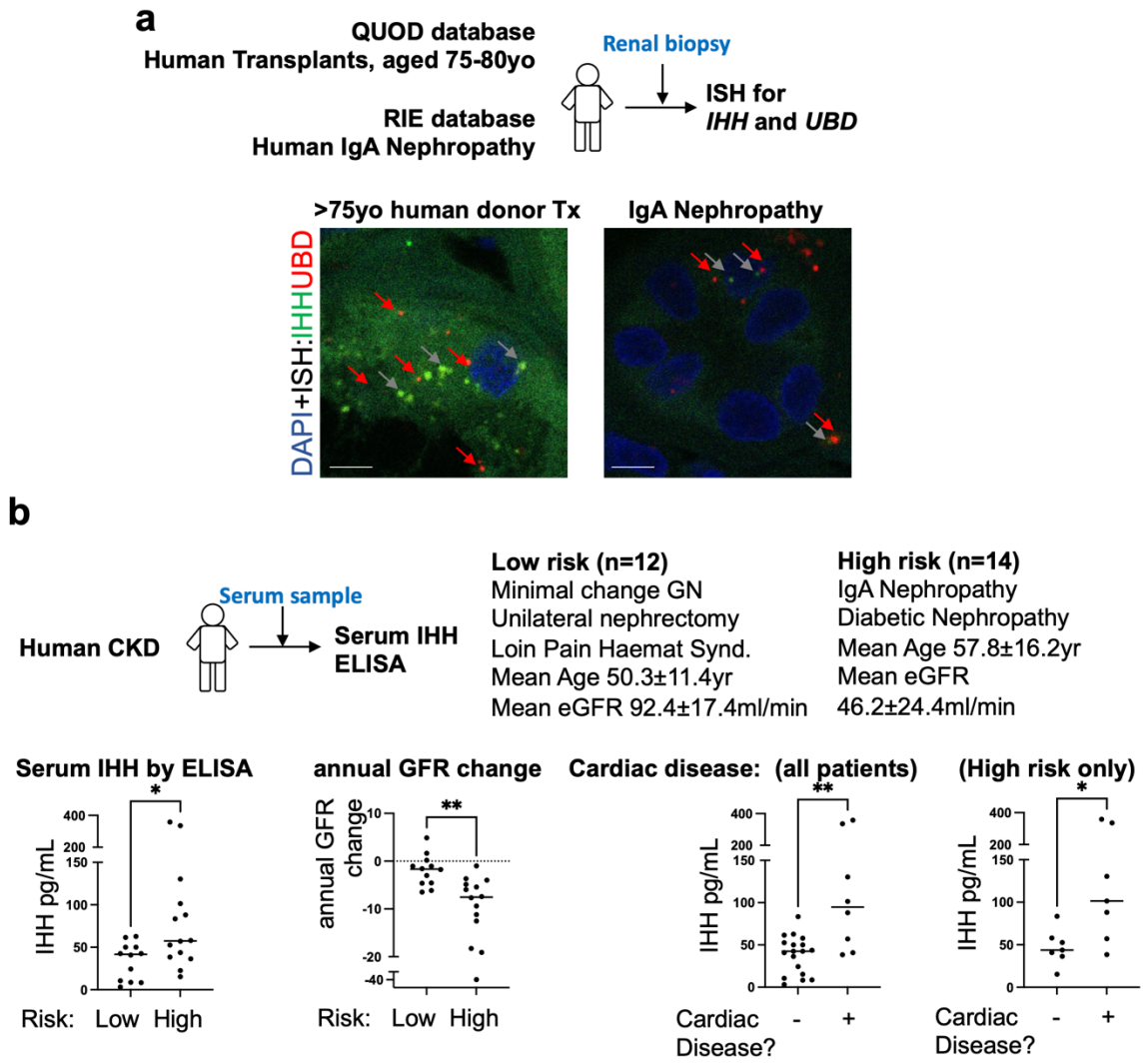

Figure 5. iPT cells and circulating IHH are increased in human chronic kidney disease

(A) Schema of studies in human tissue looking for evidence of iPT cells in human ageing and CKD. ISH for *UBD* (red arrows to red dots) and *IHH* (grey arrows to green dots) mRNA in aged (>75 years old) and diseased (IgA nephropathy) human kidneys. **(B)** Serum IHH, renal functional loss and cardiovascular disease in patients with high and low risk CKD (n=7-18/group, Mann-Whitney tests). Scale bars: 10 microns (A): Each image is representative of image acquisition and analysis performed from all experimental subjects. *p<0.05, **p<0.01, ***p<0.001, ****p<0.0001.

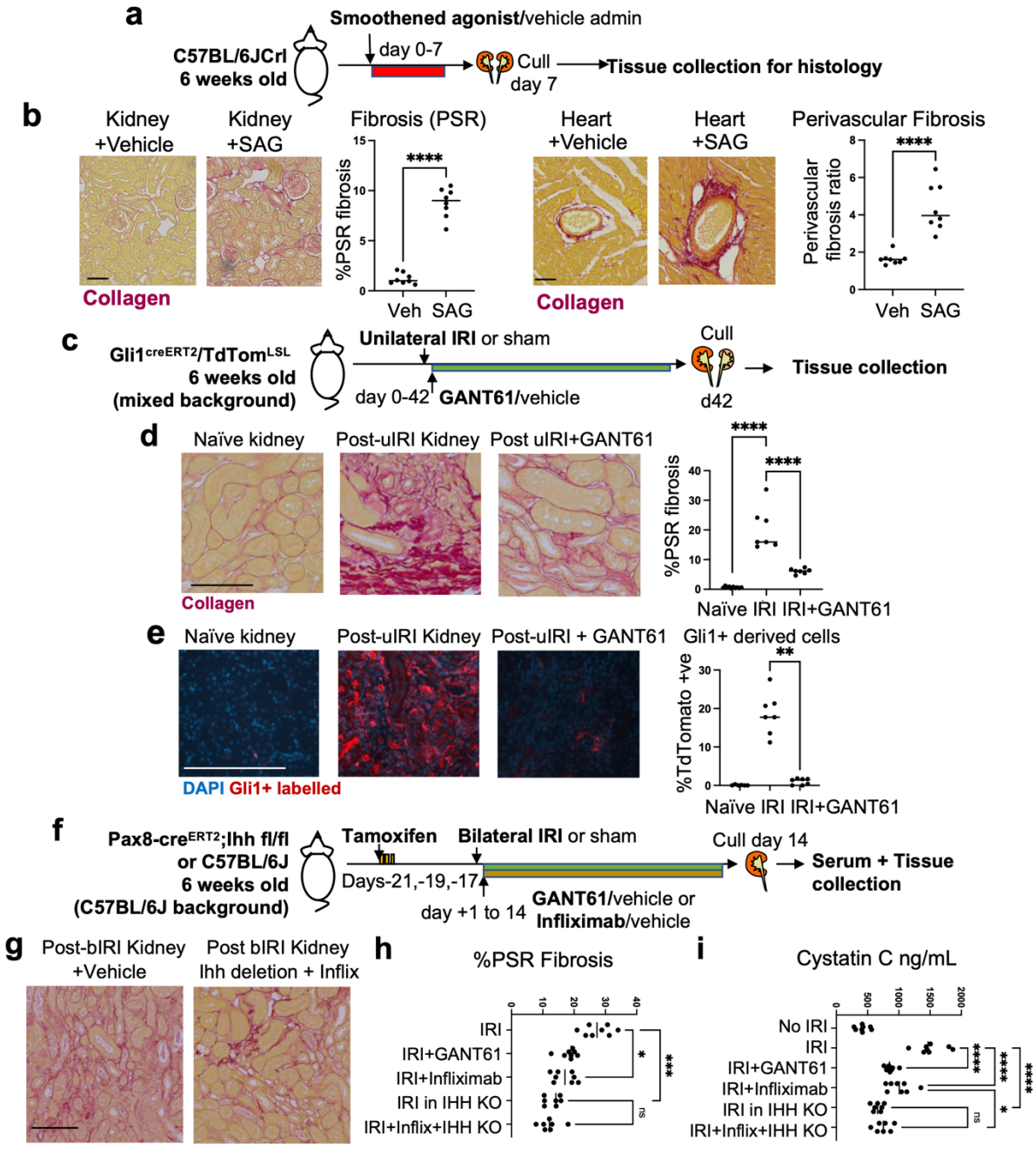

Figure 6. Pharmacological modulation of TNF and IHH signalling regulates renal fibrosis in mice. **(A)** Schema of experiments for Smoothened Agonist (SAG) administration in healthy young mice. **(B)** Images of Picrosirius Red staining and quantification of collagen (fibrosis) in the kidney and perivascular regions of the heart after SAG (n=8/group, unpaired t-test and Mann-Whitney tests). **(C)** Schema of experiments examining GANT61 treatment in Gli1-Cre TdTomato reporter mice with uIRI. **(D)** PSR staining and quantification of fibrosis after uIRI in the presence and absence of GANT61 (n=7-10/group, ANOVA with Tukey's test). **(E)**

Fluorescent imaging and quantification of TdTomato+ labelled Gli1+ derived cells in mouse kidney after IRI and GANT61 treatment. (n=6-7/group, Kruskal-Wallis test). DAPI (blue) denotes nuclei. **(F)** Schematic of experiments testing renal epithelial Ihh deletion and GANT61 or Infliximab treatment in mice with bilateral renal IRI. **(G)** Representative images of Picrosirius red staining of collagen in post-bIRI kidneys ± treatment. **(H)** Quantification of PSR fibrosis seen in panel H (n=7-8/group, Kruskal-Wallis test). Scale bars: 100microns. (**I**). Quantification of serum Cystatin C levels (n=7-8/group, ANOVA with Sidak's test). Each image is representative of image acquisition and analysis performed from all experimental subjects. *p<0.05, **p<0.01, ***p<0.001, ****p<0.0001.

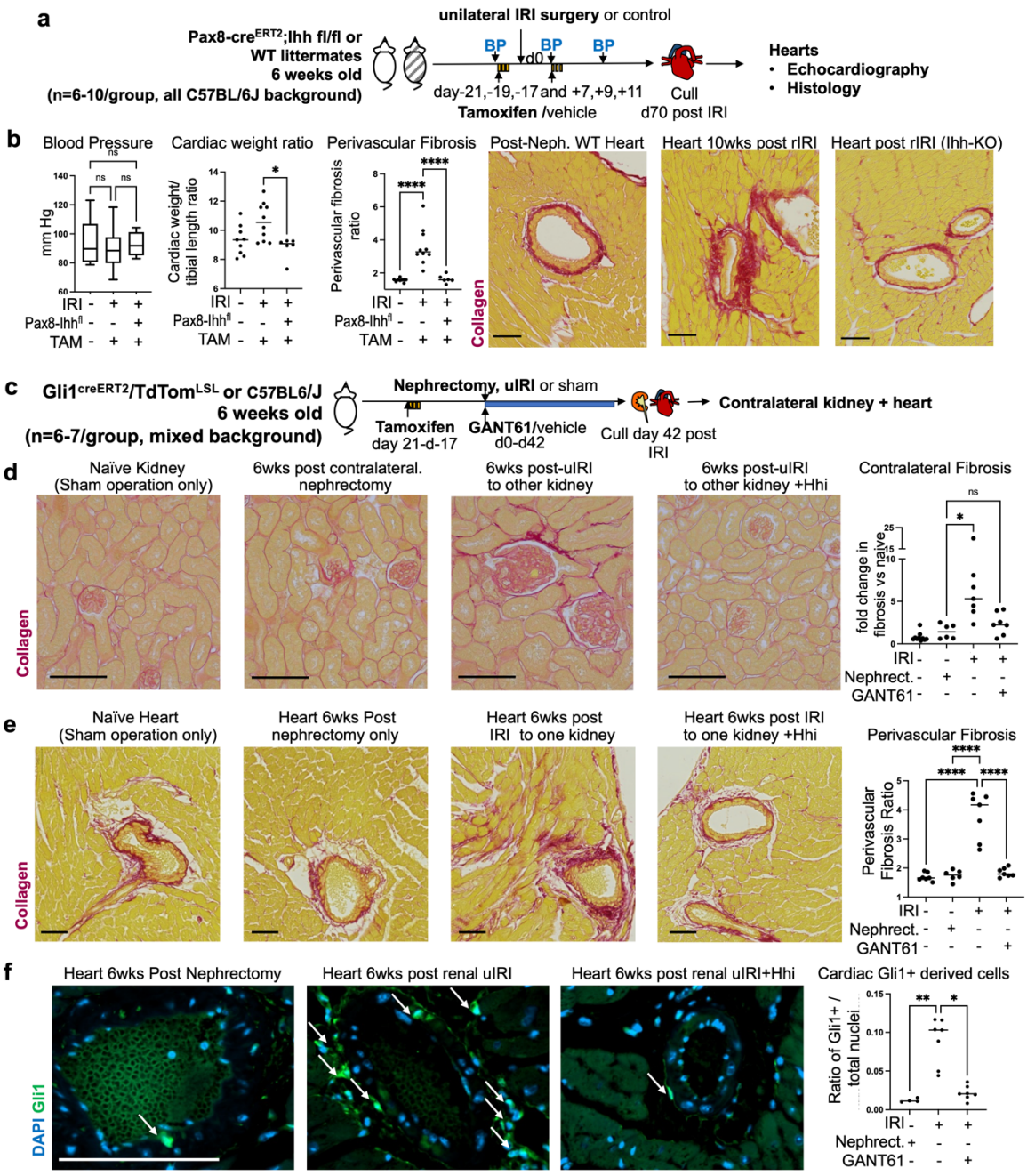

Figure 7. Inhibition of Ihh signaling limits perivascular cardiac fibrosis and Gli1+ cell expansion after uIRI in mice. (A) Schematic of experiments to examine cardiac fibrosis after conditional deletion of *Ihh* in Pax8-cre^{ERT2}; Ihh$^{fl/fl}$ mice after renal uIRI. **(B)** Quantification of blood pressure, cardiac weight/tibia length and perivascular cardiac fibrosis after uIRI (n=4-10/group, ANOVA with Tukey's or Dunnett's or Kruskal Wallis tests) Quantification of

fibrosis based on Picrosirius Red staining (representative images on right). **(C)** Schematic of experiments with Gli1-Cre TdTomato reporter mice and GANT61 treatment to examine contralateral kidneys and hearts after nephrectomy or uIRI. **(D)** Images and quantification of Picrosirius Red in the contralateral kidney after uIRI or nephrectomy (n=6-10/group, Kruskal-Wallis Test). **(E)** Images and quantification of Picrosirius Red in the heart after kidney injury (n=6-7/group, ANOVA with Dunnett's test). **(F)** Imaging and quantification of Gli1+ derived cells using AF488-conjugated antibody labelling in the heart after renal uIRI compared to nephrectomy alone (n=4-7/group, ANOVA with Dunnett's test, white arrows indicate cells derived from cells expressing Gli at the time of recombination). Scale bars: 100microns. n=6-10/group with each image representative of image acquisition and analysis performed from all experimental subjects. *$p<0.05$, **$p<0.01$.